# Polar vortices in planetary atmospheres

**Dann M. Mitchell[1,2], Richard K. Scott[3], William J. M. Seviour[4,5], Stephen I. Thomson[4], Darryn W. Waugh[6], Nicholas A. Teanby[7], Emily R. Ball[1,2]**

[1]Cabot Institute for the Environment, University of Bristol, Bristol, BS8 1SS, UK
[2]School of Geographical Sciences, University of Bristol, Bristol, BS8 1SS, UK
[3]School of Mathematics and Statistics, University of St Andrews, St Andrews, United Kingdom, UK
[4]Department of Mathematics, University of Exeter, Exeter, UK
[5]Global Systems Institute, University of Exeter, Exeter, UK
[6]Department of Earth and Planetary Sciences, The Johns Hopkins University, Baltimore, Maryland, USA
[7]School of Earth Sciences, University of Bristol, Wills Memorial Building, Queens Road, Bristol, BS8 1RJ, UK

Polar vortex, planet, exoplanet, dynamics, atmosphere

**Key Points:**

- Earth is not unique in having polar vortices, every well-observed planetary body with a substantial atmosphere appears to have at least one in each hemisphere.
- The range of planetary polar vortices in our solar system is extremely diverse, but much of their character can be explained in terms of the fluid dynamics developed for Earth.
- A novel classification of polar vortices into those with predominantly circumpolar flow (Type I) and those with large zonal asymmetries (Type II) encapsulates all polar vortex types that we know about.

Corresponding author: Dann Mitchell, d.m.mitchell@bristol.ac.uk

**Abstract**

Among the great diversity of atmospheric circulation patterns observed throughout the solar system, polar vortices stand out as a nearly ubiquitous planetary-scale phenomenon. In recent years there have been significant advances in the observation of planetary polar vortices, culminating in the fascinating discovery of Jupiter's polar vortex clusters during the Juno mission. Alongside these observational advances has been a major effort to understand polar vortex dynamics using theory, idealised and comprehensive numerical models, and laboratory experiments. Here we review our current knowledge of planetary polar vortices, highlighting both the diversity of their structures, as well as fundamental dynamical similarities. We propose a new convention of vortex classification, which adequately captures all those observed in our solar system, and demonstrates the key role of polar vortices in the global circulation, transport, and climate of all planets. We discuss where knowledge gaps remain, and the observational, experimental, and theoretical advances needed to address them. In particular, as the diversity of both solar system and exoplanetary data increases exponentially, there is now a unique opportunity to unify our understanding of polar vortices under a single dynamical framework.

## Plain Language Summary

Polar vortices are often described as the rotational motion of air in the polar regions of planets, this includes large vortices where flow circumnavigates the pole and smaller vortices that are centered within polar regions. The most commonly discussed polar vortices are those in Earth's stratosphere, which have given rise to the ozone hole. More recently a number of other circulation patterns have been described as polar vortices, on Earth, and other planets. We review key features of these different polar vortices, and explain their similarities and differences using decades of theory, observations and modelling from the geophysical fluid dynamics community. We review how the different dynamical and chemical structures evolve as features of the polar vortex structures, and why they are integral to the makeup of planetary atmospheres. We conclude by summarising the latest knowledge on potential polar vortices outside of our solar system, which to date are only theorised.

## 1 Introduction

A nearly ubiquitous feature of planetary atmospheres in the solar system are rapidly rotating flows in polar regions, that are generally referred to as polar vortices. These features may be explained by consideration of basic physical constraints. At the most fundamental level, rapidly rotating planets have a minimum of angular momentum on the axis of rotation, and a maximum at the equator. Due to their rotation, planetary bodies may be expected to develop polar cyclonic flow as a result of transport of air between different latitudes, which will tend to increase the angular momentum at high latitudes, and decrease it at low latitudes. Such transport may arise through a variety of forms, including turbulence and wave stresses or the induced circulation arising from local heating or cooling anomalies (Andrews et al., 1987).

Transport of angular momentum alone, however, cannot be used directly to determine the development of cyclonic polar motions because background rotation and density stratification combine to place further dynamical constraints on the nature of the transport. An elegant way to view these constraints is through another dynamical quantity, the potential vorticity (PV), closely related to angular momentum and its conservation. PV, q, may be defined as

$$q = \frac{\zeta_a \cdot \nabla\theta}{\rho}, \tag{1}$$

where $\zeta_a$ is the absolute vorticity vector, $\nabla\theta$ is the potential temperature gradient, and $\rho$ is the air density. The material conservation of PV on fluid particles is essentially a statement of local angular momentum conservation. In contrast to angular momentum, an atmosphere at rest has maximum PV over the pole, equal to the product of the planetary rotation rate and background density stratification (Equation 1). We refer to this resting maximum as the polar planetary PV. Material conservation of PV then implies that, again in the absence of other forces, transport alone cannot cause local PV values to increase beyond the polar planetary value. This property contains implicitly the dynamical constraints governing angular momentum transport in the presence of density stratification, at least for geostrophic flows. One consequence, for example, is that Rossby wave breaking, one of the dominant dynamical processes responsible for changes to the zonally symmetric atmosphere, may not on its own cause an increase in angular momentum (Wood & McIntyre, 2010).

To illustrate, in Earth's stratosphere the winter polar vortex is ultimately a result of local diabatic cooling in the polar night. Although such thermal forcing does not appear directly as a forcing of angular momentum, the induced circulation alters angular momentum through poleward transport, while the associated changes to the stratification lead to an associated PV increase, resulting in values significantly in excess of the polar planetary value (Andrews et al., 1987). Another way of understanding the increase in PV in terms of angular momentum transport is through the impermeability theorem, which states that the total PV between isentropic surfaces (surfaces of constant potential temperature) must be conserved, even in the presence of diabatic forcing (Haynes & McIntyre, 1990). Cooling thus leads to an increase in concentration of PV through tightening of the isentropes.

The above considerations suggest that polar vortices will always be cyclonic and dependent ultimately on the planets rate of rotation (Table 1 lists some useful planetary parameters, for comparison). Beyond that, however, there is no well-established definition for the term *polar vortex*. A polar vortex has become synonymous with multiple atmospheric features, often meaning a different thing to different communities, even for a single planet. For instance, on Earth the term polar vortex has been used to refer to three distinct atmospheric features: a stratospheric polar vortex and a tropospheric polar vortex that have strong winds that encircle the pole, as well as smaller scale tropopause polar vortices that lie in polar region (Waugh et al., 2017). Polar vortex has also been used in reference to different features on Venus (Sánchez-Lavega et al., 2017) and Saturn (Fletcher et al., 2018). These vortices have different structures, genesis, and maintenance mechanisms, but a commonality is that they correspond to coherent regions of potential vorticity. While the potential vorticity dynamics discussed above are near-universal, there are also many significant differences between the structures of planetary polar circulations, which motivates us to further refine the definition into two types, such that we employ the following definition:

| | a ($10^3$ km) | Day (Earth = 1) | Obliquity (deg) | $R_o$ | $L_d$ / a |
|---|---|---|---|---|---|
| Venus | 6.05 | 117 | 177 | 10 | 70 |
| Earth | 6.37 | 1 | 23.45 | 0.1 | 0.3 |
| Mars | 3.40 | 1.03 | 23.98 | 0.1 | 0.6 |
| Jupiter | 71.4 | 0.41 | 3.13 | 0.02 | 0.03 |
| Saturn | 60.3 | 0.44 | 26.73 | 0.06 | 0.03 |
| Uranus | 25.6 | 0.72 | 97.77 | 0.1 | 0.1 |
| Neptune | 24.8 | 0.67 | 28.32 | 0.1 | 0.1 |
| Titan | 2.58 | 16 | 27 | 2 | 10 |

**Table 1.** Planetary parameters relevant for the discussion of polar vortices. The day values are normalised to Earth. The second from last column shows the Rossby number estimated at mid-latitudes. The final column shows an estimate of the ratio of the Rossby Deformation Radius, $L_d$, to the planetary radius, a, evaluated at mid-latitudes. The obliquity values were taken from F. W. Taylor (2010) and all other values were taken from Showman et al. (2010), and readers are referred there for the full calculation and assumptions.

**A polar vortex is a coherent structure with absolute potential vorticity that is larger than the polar planetary potential vorticity, and that is centered over or near the pole. This can be split into two types:**

- **Type I: flows in which there is a predominantly circumpolar cyclonic flow. Examples include the winter polar circulations of Earth and Titan's stratosphere and Mars' lower atmosphere.**
- **Type II: flows of smaller horizontal scale in which zonal asymmetries are large enough that strong circumpolar flow is absent or of secondary importance. Examples include the Jovian vortex clusters, or synoptic-scale tropospheric polar cyclones on Earth.**

This classification is not the only possible one and even within each vortex Type, there exists a great diversity in vortex circulation patterns. On Earth, Mars and Saturn's moon, Titan, there is a single near-circular Type I vortex, with strong circumpolar winds, at the winter pole, but the detailed structure and variability differs between the vortices (D. M. Mitchell et al., 2015; Teanby et al., 2008). In general, single polar vortices also exist in each hemisphere on Saturn and Venus, but with more varied shapes: A summer-time hexagonal wave surrounds that in Saturn's northern pole (Fletcher et al., 2018), while the polar vortex core on Venus has a highly variable shape, with significant morphological changes on timescales of days (Garate-Lopez et al., 2013). In contrast to the other planets, there is not a single vortex at the poles of Jupiter but rather multiple rapidly rotating structures, with differing numbers and configuration between hemispheres (Adriani et al., 2018).

The cause of many of the differences in planetary polar vortices are not known, and there is a need for a better understanding of the fundamental processes controlling the formation, structure, and evolution of polar vortices. This is needed not only to understand the atmospheric circulation on each planet, but also to understand the atmospheric trace species chemistry. Unique transport, microphysical, and chemical processes can occur within polar vortices that result in significant differences in the composition within and outside the vortices. Perhaps, the most well-known is the ozone depletion and formation of the Antarctic ozone that occurs within Earth's stratospheric polar vortices (Farman et al., 1985). In addition, condensation (and seasonal removal of) $CO_2$ occurs within the

Martian polar vortices (Haberle et al., 2017), and there are enhanced concentrations of complex hydrocarbons and formation of ice clouds in Titan's polar vortices (Teanby et al., 2017; de Kok et al., 2014; Vinatier et al., 2018). Thus, understanding polar vortex dynamics and transport is key for understanding Earth's ozone hole, the condensation of carbon dioxide at Mars' polar ice caps, the chemistry of Titan's polar regions, and most likely microphysical-chemical processes occurring in the polar regions of other planets and exoplanets.

Here we review our current knowledge of the structure and dynamics of planetary polar vortices. In Section 2 we discuss our knowledge of Earth's polar vortices as the best observed 'archetype' of a polar vortex. In Section 3 we highlight what observations tell us about the diversity of polar vortices on other planets. In Section 4 we discuss developments in theory and idealized- through to comprehensive- numerical models which have helped to explain many of the observed features, with Section 5 also doing this for laboratory experiments. Throughout, we highlight both the diversity, as well as fundamental dynamical similarities between vortices on different planets. We discuss where knowledge gaps remain, the observational, experimental, and theoretical advances needed to address them, and, in Section 6, the possible range of vortices that may exist on the planets in other solar systems.

## 2 An archetype: Earth's stratospheric polar vortices

Earth's Type I stratospheric polar vortex is not visible to the naked eye because there are no vortex-scale cloud structures associated with it. However, the vortex has been observed using meteorological fields from multiple measuring systems; initially from stratosphere-penetrating radiosondes and rocketsondes (Gutenberg, 1949; Scherhag, 1952), but more recently from satellite measurements (Wright et al., 2021). The vortices can also be seen in satellite measurements of trace gases. Most notably, measurements of the Antarctic ozone hole that forms inside the Southern Hemisphere vortex (Schoeberl & Hartmann, 1991).

The stratospheric polar vortices are most readily characterised by strong circumpolar westerlies which maximize at around 60° latitude, from just above the tropopause (∼150 hPa) into the mesosphere (above 1 hPa; see Figure 1). These strong westerlies form in autumn when there is no solar heating in polar regions, strengthen during winter as a consequence of the large-scale temperature gradients, and then weaken and become weak easterlies in spring-summer as sunlight returns to the polar regions e.g., (Waugh & Polvani, 2010).

Historically, Earth's vortices were analyzed in terms of zonal winds or geopotential height but more dynamical insight can be gained by using potential vorticity (Hoskins et al., 1985; Andrews et al., 1987). Earth's stratosphere is highly stably stratified and mostly stable to both barotropic and baroclinic disturbances as PV generally increases in magnitude monotonically towards the pole. The polar vortices in both hemispheres have strong gradients in PV marking the vortex edge which acts as a mixing barrier between the vortex interior and the lower latitude surf zone (Figure 1b).

In the Northern Hemisphere the stable vortex state (Figure 2, left) can be disrupted by upward propagating Rossby and gravity waves. The planetary waves are generally filtered to low wavenumbers around the tropopause because higher wavenumber waves cannot propagate through the strong stratospheric westerly winds (Charney & Drazin, 1961), leading to mainly wavenumber 1 and 2 disturbances on the polar vortex (Figure 2 middle and right). These events are extreme, often causing localised heating of >70°C over a couple of days, and in many cases resulting in the complete breakdown of the polar vortex, either by displacing the polar vortex far from the pole, or splitting the parent vortex into two child vortices (Charlton & Polvani, 2007). Such events are termed

Sudden Stratospheric Warmings (Baldwin et al., 2020) and often result in tropospheric jet disturbances and associated extreme cold weather over Europe and North America (Baldwin & Dunkerton, 2001; Kolstad et al., 2010; D. M. Mitchell et al., 2013; Domeisen & Butler, 2020). However, while the causal relationship between the polar vortex breakdown and surface weather is well documented, the exact linking-mechanisms are still debated (Kidston et al., 2015).

The upward propagating waves arise, in part, due to surface orography and land-ocean contrast which are more abundant in the Northern Hemisphere. A consequence of this is that there are fewer and weaker waves in the Southern Hemisphere and the polar vortex is stronger and more stable than its northern counterpart. The seasonal lifetime of the southern vortex is longer, and there has only been one major southern Sudden Stratospheric Warming in the 60 years of observations, as opposed to ∼45 reported cases in the northern hemisphere (Krüger et al., 2005; Charlton & Polvani, 2007; Butler et al., 2017).

One consequence of the strengthened southern vortex is that the vortex edge is a strong mixing barrier, isolating polar air which allows it to get extremely cold. This results in the formation of polar stratospheric clouds throughout the vortex every winter, providing sites for heterogeneous reactions and leading to chemical destruction of ozone and formation of the Antarctic ozone hole within the vortex (Schoeberl & Hartmann, 1991). The weaker northern vortex does not get so cold, and the formation of polar stratospheric clouds and depletion of ozone is less in the northern polar vortex (Ivy et al., 2017).

The influence of Earth's polar vortex is not limited to the stratosphere, and variability in the vortex has an impact on surface weather and climate. This includes trends in Southern Hemisphere summer circulation, and associated weather, and ocean circulation, which have been linked to the ozone hole induced strengthening of the Antarctic polar vortex (Thompson et al., 2011).

Given the importance of the polar vortices on Earth, it is perhaps unsurprising how much research has focussed on them. These theoretical, modeling and laboratory studies are reviewed in Section 4, along with the links to other planetary bodies.

# 3 The diversity of polar vortices

## 3.1 Terrestrial planets in the solar system

### *3.1.1 Venus*

Mercury does not have a substantial atmosphere, so the closest planet to the Sun with polar vortices is Venus (Taylor et al., 1979). Data on the polar vortices from Venus were first collected in 1974 by Mariner 10, with a number of additional flyby and orbiter missions ever since, culminating in the Akatsuki craft making orbit in December 2015 and remaining operational ever since. While space-based missions to Venus' atmosphere have been numerous, with the atmosphere having been imaged earlier than any planet other than Earth, the longevity and sophistication of the missions have not necessarily been on par with some missions sent to Mars, Jupiter, Saturn and Titan, at least when considering the polar atmospheres.

The atmosphere of Venus is thick, with numerous cloud layers and strong superrotation (Read & Lebonnois, 2018). The Venusian atmospheric circulation has been reviewed in detail by Sánchez-Lavega et al. (2017), including a dedicated section on the polar vortices and cold collars. As noted in Sánchez-Lavega et al. (2017), the term polar vortex has been used to describe different polar features on Venus, namely a coherent hemispheric-scale swirling wind pattern (Figure 3), and a highly energetic tropical-cyclone-like vortex that precesses around the pole, and is surrounded by a region of colder

air "the cold collar" (Figure 4). Here, we refer to the former as "the polar vortex", and the latter as "the polar vortex eye". Due to the small axial tilt of Venus (Table 1), there are no strong seasonal influences, so polar vortex structures exist all year round and share many similarities between hemispheres such as depressed cloud layers inside the vortices which indicate downwelling. It was these cloud features that first pointed towards the presence of the southern polar vortex (V. Suomi, 1974; V. E. Suomi & Limaye, 1978), and later the northern one (F. W. Taylor, 2014).

At the cloud top level the southern polar vortex extends to mid-latitudes and is elliptical, which might be indicative of wave 2 planetary wave forcing (V. E. Suomi & Limaye, 1978) (Figure 3). Understanding the exact latitudinal extent of the polar vortices has proven difficult, especially given the variable vortex morphology (e.g. Figure 4). This difficulty has arisen, in part, due to the lack of in situ wind measurements (Gierasch et al., 1997), although approximations have been derived, e.g. through using thermal sounding measurements (Piccialli et al., 2012), tracking of cloud features (Limaye & Suomi, 1981), or through a full Venusian reanalysis (which are a combination of observations and atmospheric modelling to provide a holistic estimate of the climate; (Sugimoto et al., 2019)). By considering a derived zonal mean PV quantity, Piccialli et al. (2012) claimed that there was no latitude of significantly increased PV gradient at most altitudes, which would have indicated a presence of a vortex mixing barrier (i.e. a vortex edge). Their analysis was based on cyclostrophically balanced flow inferred from limited latitudinal thermal gradients, so this could have led to artificially damped PV gradients. In one region of the atmosphere, around the top of the cloud layer ($\sim$58 km), they did show some increase in the strength of the latitudinal PV gradient, and this would coincide with coherent PV structures derived from Venus Express (Garate-Lopez et al., 2016) (see also Figure 4). In both Piccialli et al. (2012) and Limaye et al. (2009) this maximum seems to be at $\sim$65°S in the southern hemisphere, although an equivalent has not been estimated for the northern hemisphere. Limaye et al. (2009) indicate that at this altitude, the vortex may be annular, although this is not observed by Piccialli et al. (2012) or in zonal mean PV analyses (Figure 1a).

Within this larger vortex structure, the most striking feature is the central core, which due to its chaotic nature sometimes appears as a dipolar 'S' shape, a monopole, or a tripole and is indicated by the bright UV regions in Figure 4. It is present in both hemispheres, but based on current data is particularly apparent in the Southern Hemisphere (Figure 4) where it rotates at a much faster rate than its northern counterpart (Piccioni et al., 2007). Analogous features are seen in Earth's tropical cyclones leading to speculation that some of the controlling factors between the two are the same, although the spatial scale and lifetimes of the two are very different (Limaye et al., 2009). For instance, while Venus' wider polar vortex structures have persisted throughout observations thereby existing for at least 40 years (and probably much longer), the more variable features in the core are generated through dynamical instabilities, lasting a couple of days, which is longer than similar features in Earth's tropical cyclones. The three orbits shown in Figure 4 reveal three very different southern vortex eye structures, but are just a small subset on Venusian morphology's that have been observed (Garate-Lopez et al., 2016).

The brighter cloud-free regions observed on Venus may indicate downwelling (Garate-Lopez et al., 2016) from the poleward and descending branches of the Hadley circulation (Luz et al., 2011), although there is still some debate in the literature over this owing to the lack of meridional wind measurements poleward of 70° (Sánchez-Lavega et al., 2017). It has been proposed that the vortices formed due to a combination of diurnal tides, and baroclinic waves (Yamamoto & Takahashi, 2015). The complex structural features of the polar vortex eyes seem to be present at multiple vertical depths, but the vortices are highly baroclinic in nature (Garate-Lopez et al., 2013, 2015, 2016).

### *3.1.2 Mars*

Mars' polar atmosphere has received more focused observations than Venus. So much so that we even have multiple reanalysis data sets (Montabone, Marsh, et al., 2014; Greybush et al., 2012; Holmes et al., 2020). Reanalysis data show that the Martian polar vortices, which extend throughout the troposphere (∼0-50 km), decrease in area with height and retain the same orientation in the vertical (D. M. Mitchell et al., 2015) (Figure 1c). A striking annular PV structure is clear in observations, reanalysis and some models, with the vortex edge coinciding with the edge of the meridional circulation (Banfield et al., 2004; D. M. Mitchell et al., 2015). Zonal averages of potential vorticity show a maximum at around 75-80°, with opposing PV gradients on either side of this maximum. This implies unstable flow (Andrews, 1987) and suggests there must be a stabilising force acting on the polar circulation.

The ring of PV is thought to form because of the latent heating due to $CO_2$ condensation inside the vortex, which decreases PV there (Toigo et al., 2017). The PV field is relatively smooth when averaged over >30 Martian days, but on shorter timescales much smaller scale PV features are apparent (Waugh et al., 2016). There is some suggestion that these features are associated with spatially inhomogeneous latent heat released during the $CO_2$ transition from gaseous to solid form, with atmospheric aerosol acting as cloud condensation nuclei (Rostami et al., 2018), but they may also be due to instabilities (Seviour et al., 2017), or simply artifacts of the reanalysis.

In most years the characteristics (e.g. size and shape) of the Martian vortex are relatively constant throughout the winter, but during years with hemispheric-scale dust storms there can be a major disruption through shifting the descending branch of the overturning circulation (Wang, 2007; Guzewich et al., 2016; Ball et al., 2021). Due to the change in dynamics and radiative absorption, "rapid polar warming" events can occur on daily timescales (D. M. Mitchell et al., 2015). A global dust storm in Martian year 28 had a particularly striking impact on the northern vortex, as seen in Figure 5a. The major growth of this dust storm likely occurred in the southern mid-latitudes, shortly before the northern winter solstice (Wang & Richardson, 2015). Zonal winds were weakened by up to 40 $ms^{-1}$ compared to a multiannual average of later years in which no global dust storm occurred (Figure 5b). Potential vorticity in the vortex was also weakened significantly, with the annulus of high PV being completely destroyed (Ball et al., 2021). Regional dust storms, which do not encircle the planet but still have high dust loading over a large area ($> 1.6\times10^6$ $km^2$) and last for multiple sols (Cantor et al., 2001), may also influence polar vortex dynamics. Large regional dust storms in the southern hemisphere have been shown to affect the northern vortex, such as the dust storm in Martian year 26 which caused the northern vortex to shrink and weaken in PV terms (Montabone, Mitchell, et al., 2014; D. M. Mitchell et al., 2015).

### *3.1.3 Titan*

Mars is not the only Solar System example of an annular polar vortex. Saturn's largest moon, Titan, also has one, with stratospheric PV peaking at around 65° latitude (Teanby et al., 2008; Achterberg et al., 2011; Sharkey et al., 2020b) (Figures 1d and 6). Since Titan orbits in Saturn's equatorial plane it shares the same seasonal variations, completing a full Titan year in ∼29.5 Earth years. Titan is tidally locked, with one hemisphere always facing Saturn, so has a day length of 15.9 Earth days, equal to its orbital period around Saturn. However, like Venus, Titan's atmosphere experiences super-rotation (Read & Lebonnois, 2018). Radiative timescales in Titan's polar stratosphere are $\sim10^7$s at 0.1 hPa, much shorter than Titan's year, allowing the vortices to respond rapidly to seasonal forcing such that they peak in strength in the winter hemisphere (Achterberg et al., 2008, 2011; Teanby et al., 2019; Vinatier et al., 2020). Due to the large Rossby

deformation radius on Titan (Table 1), the vortices are large yet still respond to perturbations as a coherent structure.

Some of the most valuable observations for understanding Titan's polar vortices are from the Cassini mission, which covers just under half a Titan year from northern mid-winter to northern summer solstice. Cassini's high orbital inclination phases allowed Titan's winter polar regions to be observed in detail, which is not possible from Earth-based observatories because Titan's winter pole faces away from the Earth (Table 1). Cassini's Composite InfraRed Spectrometer (CIRS) (F. M. Flasar et al., 2004; Nixon et al., 2019) is particularly valuable as it allows detailed measurements of temperature and trace gases directly over both poles (Achterberg et al., 2011; Teanby et al., 2019; Coustenis et al., 2020; Sharkey et al., 2020b; Sylvestre et al., 2020; Vinatier et al., 2020) (Figure 6).

Cassini observations revealed a rapid transition in the southern polar circulation direction just after northern spring equinox (Teanby et al., 2012) and the subsequent early formation stages of the south polar vortex (Teanby et al., 2017). Conversely the northern vortex was observed while fully formed and during its decline as the seasons changed from northern winter to northern summer. Modelling (Lebonnois et al., 2012) and extrapolations of the available observations (Teanby et al., 2019) suggest northern and southern vortices are similar in nature, but this has yet to be observationally verified.

The latitudinal extent of the vortices are greater on Titan than Earth and Mars (F. Flasar & Achterberg, 2008) and are almost perfectly zonally-symmetric (Sharkey et al., 2020a). Observations of trace gases in Titan's polar regions can be used to indirectly probe the circulation. Many of these gases are photochemically produced at high altitudes (i.e. above the stratosphere) and are removed by condensation in the lower stratosphere. This source-sink relationship sets up vertical gradient profiles that have increasing relative abundance with increasing altitude, with short lifetime species having stronger gradients (Teanby et al., 2009). Subsidence caused by the global overturning circulation advects enriched air down to stratospheric altitudes, causing strong enhancements in abundances that can be used to probe the atmospheric dynamics. Observations show that strong PV gradients of the vortex edge effectively isolate short-lived tracer enriched air (Sharkey et al., 2020b). For example, Figure 6c shows that $HC_3N$, which has a lifetime much less than a Titan year, is confined within the vortex. However, for longer lived species there is evidence that tongues of gas extend away from the polar vortex suggesting a role for secondary circulations or wave dynamics and instabilities in cross-boundary mixing (Teanby et al., 2008; Vinatier et al., 2020).

The polar trace gases on Titan may also play a more active role in the circulation by significantly enhancing radiative cooling at the poles. Extreme enrichment of these photochemically produced gases has been suggested to affect the radiative balance over the poles, leading to unexpectedly cold stratospheric temperatures during early winter and a potential dynamical-radiative feedback (Teanby et al., 2017). The main coolers of this highly enriched polar mesosphere are $C_3H_4$, $C_4H_2$, and $HC_3N$ (Teanby et al., 2017). These are dynamically enriched by factors of 10–1000 compared to equatorial regions, so significantly alter the radiative balance of the vortex, and may be enough to cause a sudden cooling. These extremely cold stratospheric temperatures were observed for the first time during south polar vortex formation by Cassini (Teanby et al., 2017) (Figure 6a). However, these extremely cold temperatures were not seen in the more evolved northern vortex, or indeed in the mid-winter southern vortex (Figure 6a), suggesting that subsidence-induced adiabatic heating is more important that radiative cooling once Titan's vortex is fully formed (Teanby et al., 2017). This dynamic-radiative feedback is so far thought to be unique to Titan; on Earth (and indeed Mars and Venus) this is not the case, as $CO_2$ is the dominant radiative cooling agent, which is well mixed and so not redistributed and concentrated into subsiding polar regions in the same way (Teanby et al., 2017).

### 3.2 Gas giant planets in the solar system

Polar vortices are not unique to terrestrial planetary bodies; we have observed them on all four of the solar system giant planets (Figure 3). We have known about the polar vortices on Saturn, Uranus and Neptune for decades, because ground-based telescopes have been able to observe them during the relevant seasons. This is only possible because the obliquity of these planets is large, in all cases greater than 25° (see Table 1).

#### *3.2.1 Jupiter*

Jupiter, with an obliquity of ∼3°, however, has only very recently had its polar region observed during polar orbits of the Juno probe (Bolton et al., 2017). Other missions flying by the planet were confined to Jupiter's equatorial plane, so suffered the same limitations as Earth-based measurements. The Juno spacecraft was able to view Jupiter's polar regions for the first time, using both visible and infrared (IR) sensors, and revealed a fascinating and unexpected Type II vortex at both poles. Located ∼0.5° offset from the North Pole, there exists a central, cyclonic vortex consisting of small-scale cloud structures (Figure 3). The central vortex is surrounded by eight cyclonic vortices of similar diameter (4000-4500 km) that are likely to have similar rotation rates around their axis of rotation, as the central vortex rotation does, ranging from ∼26-60 hours, depending on the vortex. However, given observational uncertainty, there may be some progressive motion (Adriani et al., 2018). The eight surrounding vortices form a quadrilateral structure with each side being composed of a line of 3 vortices which alternate between cloudier and clearer structures (Figure 3).

The southern polar vortex only contains five vortices surrounding a central vortex. The vortices are larger in diameter by ∼1500 km than those of the Northern Hemisphere, but are more spaced out, with clear gaps between the vortices filled with meso-scale wave and jet structures (see, for instance Figure 1 in (Adriani et al., 2018)). The central southern vortex has clearer cloud banding than its Northern counterpart, and the core of the vortex is far more elliptical than any of the other vortices (Adriani et al., 2018). Unlike in the Northern Hemisphere, there is a clear counter-clockwise progressive motion of the five surrounding vortices relative to the central vortex's rotation speed.

With only a single targeted mission to observe Jupiter's atmosphere, it is hard to discern the vertical extent of the polar vortices, and as such it is not obvious which layers of the atmosphere these exist in, or whether the structure is barotropic or baroclinic in nature. As the observations are currently from visible and IR sensors, they are mainly looking at the cloud 'tropospheric' layer, although this does not preclude vortices at other levels in the atmosphere. With such a short observation period it is not clear how these vortex clusters will change with time, although the currently observed period suggests some migration of the vortices. The existence of stable Northern and Southern polar vortices at the same time is unusual for planets, although due to its axial tilt Jupiter does not really experience seasons and seasonality on other planets is often associated with the forming and breakdown of polar vortices, i.e. through changes in latitudinal temperature gradients.

#### *3.2.2 Saturn*

Unlike on Jupiter, the polar vortices in Saturn's stratosphere (∼200-300 km above the cloud layer) are seasonal, but in the opposite sense to Earth, such that they are established before the summer and breakdown before winter (Orton & Yanamandra-Fisher, 2005; Fletcher et al., 2008). The Cassini probe has allowed us to observe Saturn's polar circulation in unprecedented detail (Baines et al., 2009; Sayanagi et al., 2018). As with most other known planetary polar vortices, a single Type I vortex exists centred on each pole, but smaller (typically 1000-1500 km in diameter) cyclonic and anti-cyclonic

features are also observed (Antuñano et al., 2018), reminiscent of Type II vortices, and these can be seen as bright spots in Figure 3. Both of Saturn's stratospheric polar vortices are circular in nature, with the polar vortex edge reaching speeds of 140-160 $ms^{-1}$ (Antuñano et al., 2015; Sayanagi et al., 2017). The peak potential vorticity in both hemispheres is at the pole, with the southern polar vortex exhibiting higher absolute values (Antuñano et al., 2019).

A distinctive feature in the northern hemisphere is that the vortex is surrounded by a zonal wavenumber-6 'hexagonal' westerly jet which peaks at around 100 $ms^{-1}$. This jet was observed by Voyager in 1980 (Godfrey, 1988), and has persisted ever since, most likely resulting in two strong PV gradients within the polar region that constitute the strong cyclone vortex, and a nearby jet (Figure 3) (Scott & Polvani, 2006; Fletcher et al., 2018; Antuñano et al., 2019). While there exists a jet at a similar latitude in the southern hemisphere, it is weaker (Sayanagi et al., 2018), and does not have the same wavenumber-6 pattern, despite having similar potential vorticity gradients (and as such potential for instabilities) (Antuñano et al., 2019).

The polar vortices exist for >100 km in the vertical, covering both the stratosphere and troposphere, but it is not currently known how far below the visible cloud layer they extend (Sayanagi et al., 2018). The tropospheric polar vortices share many similar characteristics of the stratospheric ones, but importantly are present all year round, still with similar strengths though (Dyudina et al., 2008). In the Northern Hemisphere, the tropospheric polar vortex again has a close-by hexagonal jet (Allison et al., 1990). The tropospheric vortex is highly convective, with an inner and outer eyewall of cloud extending to the tropopause (Dyudina et al., 2008). As with the other gas planets, the vortices on Saturn are associated with a warm polar region (Orton & Yanamandra-Fisher, 2005; Dyudina et al., 2009). There is a suggestion that within these polar vortices subsidence takes place, as evidenced from increased optical thicknesses of the stratospheric hazes and the location of the base of the tropospheric haze (Sanz-Requena et al., 2018).

#### *3.2.3 Uranus and Neptune*

The polar regions on the icy giants Uranus and Neptune are less well studied because there have been no high-inclination space missions equivalent to Juno or Cassini for these planets, with only the single Voyager 2 flybys in 1986 and 1989 respectively. The Voyager observations of the polar regions are augmented with ground-based telescopic observations, with advances in adaptive optics and radio interferometry affording detailed if sometimes rather oblique polar views (de Pater et al., 2014). Using the available observations, the strongest evidence of polar vortices comes from identifying polar clouds. Such features are observed in Uranus' southern polar region, with a symmetric vortex centred slightly off the pole, rotating with a period of ∼24 hours and extending out to 84°S (Karkoschka, 2015). Uranus' North polar region also clearly has cloud or haze features (de Pater et al., 2015; Sromovsky et al., 2012) but no corresponding vortex edge is observed (Figure 3), suggesting Uranian vortices may be a seasonal phenomenon like on most other planets (Sanders, 2017; Brueshaber et al., 2019).

Neptune's north polar region has been particularly difficult to observe due to its axial tilt shadowing it from Earth for a number of decades (Table 1), meaning the circulation features cannot be tracked (Karkoschka, 2015). However, in the Southern Hemisphere, a bright polar cloud structure has been observed which resembles the convective polar vortices on Saturn (Fletcher et al., 2015, 2012), and which has persisted since the Voyager era, far longer than other convective systems at lower latitudes on Neptune (Luszcz-Cook et al., 2010; Irwin et al., 2016). It has been reported that this region constituted a hot pole, and argued that it was due to seasonal heating (Orton et al., 2007), although it could also be a hole in the clouds, allowing for detection of warmer regions of the atmosphere. As with Jupiter and Saturn, it is likely that this is a stable polar vortex, but

unlike those planets, the polar vortex on Neptune is significantly larger in latitudinal extent, with the edge located at ∼80°S (Luszcz-Cook et al., 2010).

## 4 Theory and modelling

Observations can only take us so far in our understanding of planetary polar vortices, in part because there are many aspects of a planetary system we cannot directly observe but also because it is not possible to test the controlling factors of the system by switching on or off certain processes or 'forcings'. It is therefore necessary to combine observations with theory and a hierarchy of models to develop a fuller understanding of the polar vortices (Figure 7). In this section we give an overview of a range of complexity of models that can be used to understand polar vortices in some way. These range from very idealised models used to understand the basics of vortex dynamics, through to comprehensive models of individual planetary polar vortices.

Perhaps the simplest representation of a polar vortex is as a region of uniform potential vorticity, or 'vortex patch'. Studies date back to Kirchhoff (Kirchhoff, 1876), with the original vortex stability results (Love, 1893) and sheared vortex regimes (Kida, 1981) still just as relevant today in understanding the stability of monopolar PV distributions, such as Earth's stratospheric polar vortex (Matthewman & Esler, 2011). Elliptical perturbations to the vortex edge may be readily generalized to any azimuthal wavenumber: the vortex patch again provides a convenient model for the study of finite amplitude Rossby waves on the edges of monopolar vortices and the dynamics of wave breaking (Dritschel, 1986; Waugh & Dritschel, 1991; Polvani & Plumb, 1992).

Another straightforward generalization of the vortex patch model, relevant to cases of non-monopolar polar vortices, is by considering an annular distribution of uniform potential vorticity in which the potential vorticity maximum is located at a finite radius from the pole. Such configurations tend to be dynamically unstable. The linear stability of the equivalent distribution in planar Cartesian geometry, comprising a uniform strip of vorticity, was described originally by (Rayleigh, 1880). The original analysis has been subsequently modified to include the effects of nonlinearity and spherical geometry (Dritschel & Polvani, 1992) (Fig 7a) as well as the effect of finite deformation radius (Waugh & Dritschel, 1991).

In both monopolar patch and annulus cases, the extension from two to three dimensions is straightforward, if computationally more expensive. To the extent that many of the dominant dynamical processes are layerwise two-dimensional, the two-dimensional models still provide a useful dynamical framework in which to test hypotheses in many cases of interest. The idealization of uniform potential vorticity inside and outside the patch or annulus can be easily generalized to continuous distributions. The annulus model was recently used to study the growth of disturbances in the context of the annular Martian polar vortex, which can be viewed, for example, as resulting from a competition between dynamical instability and the restoring effects of radiative forcing (Seviour et al., 2017; Rostami et al., 2018; Scott et al., 2020). Another application is to the hexagonal wave structure observed near Saturn's pole. While the hexagon exists on a jet surrounding the more compact polar vortex at its centre, rather than the polar vortex itself, its development may again be examined in terms of the basic two-dimensional potential vorticity distributions. The simplest description is that of a wave on the edge of a vortex patch, following Deem and Zabusky (1978); Polvani and Dritschel (1993), though perhaps a more realistical picture is given in terms of the instability of an annular structure coupled to a central patch (Rostami et al., 2017).

In a similar way, the study of arrays of vortex patches or point vortices, and the motions of single patches on a background planetary vorticity gradient can provide insight into the polar vortices on the gas giants. Polar cyclones on Saturn, Uranus and Nep-

tune may all be expected to arise under very general conditions as a result of vortex beta-drift, whereby coherent cyclones induce circulation patterns that result in a net poleward drift of the cyclone (Lam & Dritschel, 2001; O'Neill et al., 2016). This is of course also true for terrestrial planets, although often in the troposphere friction prevents vortices from reaching the pole. For instance, analogous to tropical cyclone drift to mid-latitudes on Earth. For Saturn, the poleward drift and subsequent merging of cyclones was demonstrated to result in persistent polar accumulation of cyclonic vorticity under general conditions and with no external forcings (Dyudina et al., 2008, 2009; Baines et al., 2009). Cyclones will migrate to the pole if their initial strength exceeds the potential vorticity at the pole by about 12% (Scott, 2011), a constraint that effectively limits polar accumulation to vortices originally relatively close to the pole. The speed of poleward migration is slower at smaller planetary Rossby deformation radius, $L_d$, which already gives a key to different in planetary polar vortices (Table 1). A closely related parameter, the planetary Burger number $Br = (L_d/a)^2$, where $a$ is the planetary radius, has also been shown to be a key parameter controlling polar vortex regimes (M. E. O'Neill et al., 2015). When varied in conjunction with an energy potential parameter (this energy could take the form of, e.g. latent heat), then vortices that share characteristics of those observed on other planets can be established. Notably if the energy parameter is too small then cyclones cannot reach the pole before their energy is radiated away in the form of Rossby waves.

An attempt at fitting Jupiter's vortices into this dynamical framework was subsequently undertaken (Brueshaber et al., 2019) and two additionally controlling parameters were found (albeit less important than the Burger number). These were the initial cyclone strength, and the ratio of the number of initial cyclones versus initial anticyclones. These additional parameters were found to modify the transitions between different giant planet polar dynamical regimes, namely ice-giants and Saturn, but also to some extent Jupiter, although the observed configuration (Adriani et al., 2018) was not fully reproduced. Insight into the multiple vortex configurations on Jupiter can also be drawn from existing stability criteria obtained for arrays of point vortices or patches. While the original observations of the Jovian vortex arrays generated a certain degree of excitement, theoretical studies of the stability of such configurations date back to (Thomson, 1883), who showed that an array of up to five regularly spaced point vortices forms a stable configuration. Since then numerous studies have extended Thomson's result by considering, for example, background shear or the addition of a central vortex, both of which have a stabilizing effect (Schecter et al., 1999; Fine et al., 1995). A recent example in which a stable ring of vortices surrounds a central one in a Boussinesq atmosphere is shown in Figure 7d (Reinaud & Dritschel, 2019), although from these examples it is unclear as to why these clusters may form on Jupiter, but not the other gas giants.

The natural tendency of migrating vortices to merge at the pole is clearly not happening on Jupiter, and it is likely that each Jovian cyclonic vortex is 'shielded' by a band of anti-cyclonic air on the vortex edge, acting to repel the sibling vortices (Li et al., 2020). Figure 8 show a shallow water simulation of this process as an example of how it may happen on Jupiter. An intruding shielded vortex migrates from low latitudes and reaches the cluster at day 17, rotating around the Type II polar vortex cluster until it finds a way in at around day 58, ultimately forming a new stable configuration. This type of process could explain the different numbers of vortices at Jupiter's two poles, as well as the recently observed vortex migration.

From the combined theory and modelling discussed above, a natural question then arises: what aspects of polar vortices can be understood in terms of the freely evolving, unforced dynamics alone, and what aspects are intrinsically related to dynamical or thermodynamical forcings present in the system? A suitable system for addressing this is the single-layer shallow water model, or its quasi-geostropic approximation, representing the quasi-horizontal dynamics between two isentropic surfaces. Such a model may capture

the most relevant motions in a shallow atmosphere when $f/N$ is large (where $f$ is the Coriolis parameter, and $N$ the Brunt–Väisälä frequency), possibly with additional explicit forcings to represent the effects of parts of the atmosphere outside the layer of interest; the use of such forcings thus allows some fully three-dimensional effects to be included. The shallow atmosphere model has a long history of applications to the Earth's winter stratospheric polar vortex, where many ideas of mixing and transport, surf zone formation, gradient intensification and the formation of transport barriers, have all been convincingly illustrated and analyzed (Polvani et al., 1995; Juckes, 1989) and it also captures some of the key features of certain vortex breakdown events (Rong & Waugh, 2004; Matthewman & Esler, 2011; Liu & Scott, 2015). In these cases, the appropriate forcings are a relaxation on the layer thickness, representing the effects of radiative cooling in the polar night, and a bottom wave perturbation, representing the combined effects of all upward planetary wave propagation from the troposphere.

Non-Earth polar vortices may be forced in much the same way, with appropriate choice of radiative equilibrium and wave forcing. This approach was adopted recently to examine the persistence and dynamical stability of the annular polar vortex on Mars (e.g. Figure 7b), considering under what conditions such a vortex may persist in an approximately zonally symmetric state, or alternatively break up transiently into a more eddy dominated regime (Seviour et al., 2017; Rostami et al., 2018). Different regimes are found to be governed by the strength of the annular forcing, the radiative relaxation timescale, as well as details of topographic forcing. Mixing and transport are altered dramatically according to the regime and so understanding persistence is key to understanding atmospheric composition on Mars, and more generally on atmospheres with similar annular structures. Titan's polar vortex is a key example here, with radiatively active tracer isolation and subsidence inside the vortex being key to its development and evolution (Teanby et al., 2017).

While the radiative forcing used by Seviour et al. (2017) is a natural and convenient way of forcing the basic annular structure, an alternative is to represent the latitudinal transport of angular momentum by the Hadley cell outflow, which on Mars and Titan can extend to 60° (Figure 3) latitude or beyond in the northern hemisphere winters (Waugh et al., 2016; Teanby et al., 2019; Sharkey et al., 2020a). Again, while the Hadley cell itself is an intrinsically three-dimensional circulation, it may be represented in the shallow water model by an appropriate mass source/sink in the layer thickness (Shell & Held, 2004). This approach was adapted to the Mars regime by allowing a stronger and more asymmetric Hadley cell (Scott et al., 2020). The advantage is that it captures the zero potential vorticity of the angular momentum conserving circulation in a natural way (Held & Hou, 1980). Meanwhile, latent heat release from carbon dioxide deposition over the winter pole alters the polar potential vorticity (Toigo et al., 2017) and the effects of the two processes on the annular distribution can be analyzed in isolation.

Moving towards more complex models, a large number of studies have investigated polar vortices in stratified atmospheres using three-dimensional integrations of the primitive equations (Figure 7e). In their simplest form, these consist of a Newtonian thermal relaxation towards a specified temperature profile, in place of an explicit representation of radiation (Held & Suarez, 1994). Such relaxation schemes have been adapted for application to Earth's polar stratosphere (Polvani & Kushner, 2002; Jucker et al., 2014) and are able to capture a realistic vortex climatology, as well as both split and displacement sudden stratospheric warming events (Gerber & Polvani, 2009). By varying surface topographic and surface heating forcings, as well as lower-stratospheric winds, within such simulations, studies have made progress in explaining the observed seasonality and inter-hemispheric differences in the frequency of sudden stratospheric warmings (Sheshadri et al., 2015; Martineau et al., 2018; Lindgren et al., 2018; Scott & Polvani, 2006). Similar Newtonian relaxation schemes have been applied to the atmospheres of Venus (Yamamoto & Takahashi, 2006; Lee et al., 2007, 2010), with Lee et al. (2010) in particular simulat-

ing the hemispheric polar vortex and associated spiral arms seen in observations, and Mars (Collins & James, 1995; Haberle et al., 1997; Thomson & Vallis, 2019b), with the addition of a temperature lower bound to represent $CO_2$ condensation. While these studies produced relatively realistic polar zonal winds, they have not focused in detail on polar vortex structure.

At the top of the hierarchy of model complexity sit comprehensive general circulation models (GCMs; Figure 7f), which include both a radiation scheme, parameterisations for subgrid-scale processes such as convection and clouds, and possibly a coupled ocean and interactive atmospheric chemistry. In recent years many Earth GCMs have moved towards increased vertical resolution in the stratosphere, leading to an improvement in their representation of the stratospheric polar vortex and its variability (Charlton-Perez et al., 2013). Despite this, there remain longstanding biases including too few sudden stratospheric warming events in most models (Charlton & Polvani, 2007), as well as an underestimate of the relative frequency of split vortex (or zonal wavenumber-2) events (Seviour et al., 2016) (though it should be noted that biases vary widely between models). Importantly, GCMs are used to understand how vortex variability may vary under climate change, an area of research where great uncertainty remains (see Baldwin et al. (2020), for a detailed discussion). Some Martian GCMs include comprehensive representations of the global dust cycle and dust aerosol properties, with many GCMs able to simulate prescribed or freely-evolving dust storms, and $CO_2$ condensation which both play significant roles in polar vortex dynamics, as discussed in Section 3. Indeed, Toigo et al. (2017) showed that if the process of $CO_2$ condensation is turned off in their GCM, the vortex took on a monopolar, rather than annular PV stucture, and so argued that it is this process which leads to the observed annulus. Ball et al. (2021) showed that with the inclusion of dust in an idealized Martian GCM the mean-state and variability of the northern Martian polar vortex were significantly better captured. Titan GCMs have been developed to include a representation of the methane cycle (Lora et al., 2015), and have been applied to simulate the tropospheric and stratospheric circulations, though modelling studies have not focussed explicitly on polar vortex structure. There are, in addition, great uncertainties when comparing existing Titan GCMs (Lora et al., 2019; Lebonnois et al., 2012), particularly in the strength of extratropical zonal winds and the degree of superrotation (Newman et al., 2011). Continued improvement in the simulation of planetary polar vortices will necessitate more detailed inclusion of important physical processes in GCMs, while at the same time gaining physical insight and understanding from the use of more idealised models.

## 5 Polar vortices in the laboratory

Laboratory studies provide an alternative type of model which complements those discussed in Section 4 (Figure 7c). Perhaps the most common type of laboratory study concerned with large-scale atmospheric dynamics is the thermally-driven rotating annulus experiment, on which there is a vast literature that we do not completely review here, where a rotating cylinder of fluid is cooled at the inner boundary and heated at the outer boundary, representing the differential heating of a planet by its star (e.g. (Hide, 1953; Fultz et al., 1959)). Thermally-driven rotating annulus experiments have mostly been concerned with studying regimes of baroclinically unstable situations, perhaps most relevant to midlatitude on Earth and other planets. For example, transitions are typically observed from axisymmetric overturning Hadley-cells, through weakly-nonlinear wave-like regimes to full geostrophic turbulence with multiple jets as parameters are changed (e.g. (Hide & Mason, 1970; Hart, 1972; Hide & Mason, 1975; Spence & Fultz, 1977; Bastin & Read, 1998; Read, 2011)). Such baroclinic-wave-like behaviour and interactions with the overturning circulation are perhaps most relevant for polar vortices like those on Mars, whose baroclinic wave-like behaviour has been compared with the wave-like regimes in rotating annuli (Collins & James, 1995), although there are certainly parallels to be drawn

between the wave dynamics observed in annulus experiments, and the waves typically found on the polar vortex edge on Earth. One weakness of using such experiments for studies of polar vortices specifically is that they necessarily contain some kind of central barrier near the axis of rotation (normally used to contain a source of cooling to drive horizontal motion within the annulus). Such a barrier therefore prevents a vortex forming right over the pole. Experiments forced in other ways can remove the need for such a central column, and thus study jet formation and polar vortex formation in polar regions. One particular example of this is the experiment of (Y. Afanasyev & Wells, 2005), which is a rectangular rotating tank with a cylindrical insert, and is forced by an initial array of vortex dipoles created through the combination of electrical currents and an array of magnets. Such a setup is found to produce circumpolar jet streams, and displays a PV maximum over the pole, and a wavy jet edge, somewhat reminiscent of a typical Type I vortex (see e.g. figure 2a of (Y. Afanasyev & Wells, 2005)). Varying the rotation rate of such an experiment allows vortex properties to be compared across different regimes, with smaller values of $\beta$ producing a more isotropic region of chaotically-interacting circular vortices. For a more general discussion of experiments of this kind, see (Y. D. Afanasyev, 2019).

For planets where the thermally-driven meridional overturning circulation is not connected to the polar vortex, e.g. those on the giant planets, the thermally-driven annulus experiments are perhaps less relevant. There are a relatively small number of studies, however, that have investigated such polar vortices in laboratory experiments. A key example is the study of Saturn's polar hexagon (Aguiar et al., 2010) (see also Figure 7c), with other more generalised examples also providing relevant insight (Montabone, Wordsworth, Aguiar, Jacoby, Read, et al., 2010; Montabone, Wordsworth, Aguiar, Jacoby, Manfrin, et al., 2010). These studies use rotating tanks without any differential heating. They are based on the idea that the wave-like polygonal shapes around polar vortices are a manifestation of barotropic instability. Others have used a differentially rotating section of their tank's upper lid to spin up a barotropically unstable jet (Aguiar et al., 2010). They find regimes where wave-like perturbations are superposed on the jet, which saturate at finite amplitude, with the wavenumber of the perturbation depending on their parameters. Although they cannot approach Saturnian parameters with all of their control parameters, a Saturn-like Rossby number can be attained, and this regime shows a preference for hexagonal wave-6 waves. Similar results have also been found in other studies (Montabone, Wordsworth, Aguiar, Jacoby, Read, et al., 2010; Montabone, Wordsworth, Aguiar, Jacoby, Manfrin, et al., 2010), but in a setup where their vortex is created by having a sink of fluid over the centre of their tank. They also find low-wavenumber perturbations to the vortices that share some similarities with perturbations seen on Earth, Venus and Saturn. More recent numerical work has suggested that perhaps the presence of a polar vortex over the pole is important to produce a more Saturn-like hexagon than is produced in these lab experiments (Rostami et al., 2017), but in essence the paper highlights the same mechanism - namely that barotropic instability is able to generate the hexagonal pattern.

One weakness, perhaps, of past laboratory experiments studying polar vortices on giant planets is that they do not readily include the poleward migration of small vortices that may be relevant for forming polar vortices (as described in section 4). To include such effects in a lab experiment would require the representation of the $\beta$ effect, and a mechanism for producing small vortices. As is well-known, the $\beta$ effect can be represented through the use of either a sloping bottom boundary (when using a fixed-upper lid), or by utilising the parabolic shape adopted by a rotating mass of fluid with a free upper surface. It is possible to represent small-scale moist convection in lab experiments using saline injections (e.g. (Read et al., 2004)), vertical forcing through the use of magnets (e.g. (Y. Afanasyev & Wells, 2005)), and of course small vortices can be generated through thermally-driven convection (e.g. in rotating annuli). Perhaps one future direction for laboratory experiments relating to polar vortices would be to attempt to rep-

resent both the barotropic-instability of polar jet streams and the poleward migration of small vortices, with the hope that the interaction of these mechanisms could be better understood.

A significant insight gained from laboratory experiments is the utility of regime diagrams, which are commonly used to describe the flow behaviour as a function of parameters in laboratory experiments (Read, 2011). These have recently proved insightful when describing regimes of behaviour in global circulation model experiments using non-dimensional (Wang et al., 2018; Thomson & Vallis, 2019a), or dimensional parameters (Kaspi & Showman, 2015; Komacek & Abbot, 2019). As studies of planetary polar vortices are extended to wider parameter ranges, such regime diagrams may also prove useful for understanding polar vortex behaviours over a range of planetary attributes.

## 6 Thinking beyond our solar system

Given that over 4000 exoplanets have been discovered to date, many with substantial atmospheres (NASA Exoplanet Archive: doi:10.26133/NEA1), the polar vortices in our solar system are likely to represent only a small subset of polar vortices that could exist in a planetary atmosphere. If Earth were an exoplanet, our current infrared measurements would observe the upper atmosphere, namely the stratosphere and mesosphere, but not the troposphere. Polar circulations in these regions are particularly important because they can redistribute atmospheric constituents, depending on how stable they are. Observation-based estimates of the zonal wind speed for planetary bodies outside the solar system exist, for instance, on brown dwarfs, which are hypothesised to have polar vortex-dominated regimes (Apai et al., 2021). By comparing the period of the infrared emissions from the upper atmosphere, with the period of the radio emissions from the planet interior, Allers et al. (2020) estimated that their chosen brown dwarf had strong westerlies of $650 \pm 310$ ms$^{-1}$, although subsequent modelling studies have not been able to capture the magnitude of these winds (Tan & Showman, 2021).

Due to the nature of the detection methods used, the known exoplanets are normally very close to their parent star and have very fast orbital periods, often equivalent to 5-35 Earth days. One consequence of this is that tidal forces are stronger, often resulting in the planetary rotation rate and orbital periods synchronising, which puts their atmospheres into very different regimes than those observed in our solar system. These are known as tidally locked regimes, and the majority of exoplanet atmospheric dynamics studies have focussed on this regime type.

To date, there have been no targeted studies modelling polar vortices on exoplanets but there have been a number of studies looking at other features of planetary atmospheric circulation, notably either atmospheric winds in a general sense, or the Hadley circulation which is a controlling factor for some polar vortices. In the context of exoplanets, these studies generally fall into two categories. The first are targeted studies of a specific exoplanet atmosphere. The most common systems studied are TRAPPIST and Proxima Centuri, as those have been some of the most observed and have high chances of Earth-like planets. While not all necessary atmospheric boundary conditions to run GCMs of exoplanets are yet measurable, Fauchez et al. (2020) modelled the atmospheric circulation of TRAPPIST-1e using plausible assumptions of the unknown parameters. Here we show their data re-plotted to focus on the polar region (Figure 9), where a polar vortex with strong zonal winds (50-60 ms$^{-1}$) exists, with cold polar temperatures, much like some of the vortices described in Section 3. However, polar vortices do not always exist, and Carone et al. (2015) showed that polar tropospheric jets were possible for some tidally locked planets with specific planetary parameters. However, these did not exist on planets with longer orbital periods, in which cases radial flow dominated over the zonal flows. The relationship is more apparent for larger planets, for instance some of those in the Proxima Centuri system. Expanding on their earlier work, Carone et al.

(2018) specifically look at the stratospheric circulation on exoplanets within the TRAPPIST and Proxima Centuri, and identify weak polar jets in both hemispheres at the same time, but only when the stratospheric overturning circulation was dominated by extratropical vertical Rossby wave activity. If instead it is dominated by tropical wave activity, the jets were not established.

The second category of exoplanetary analysis is focussed more on the idealised nature of atmospheric regimes to changes in planetary parameters, such as the planetary rotation rate, or planetary radius, rather than modelling a specific exoplanet. These studies consider both tidally locked, and freely rotating exoplanets, and show in both cases that tropospheric jets can form in the polar regions for Earth-sized exoplanets (Edson et al., 2011). Again, these studies do not explicitly focus on the polar vortices, but we can infer some characteristics from other circulation diagnostics. For instance, a body of research shows that the width of the Hadley cell has a strong dependence on the planetary rotation rate and radius, with the cell extending further poleward for slower rotating planets, or smaller radii planets (Held & Hou, 1980; Kaspi & Showman, 2015; Komacek & Abbot, 2019). The atmospheric cloud particle size has a secondary effect, with larger particles giving rise to a more vigorous atmospheric circulation, which will be especially important for planets with convectively active polar vortices, such as the solar system gas-giants (Komacek & Abbot, 2019). The atmospheric mass of the planet is another key parameter that is strongly correlated with the strength of the Hadley Cell, with thicker atmospheres giving rise to stronger poleward transport (Chemke & Kaspi, 2017).

Importantly, almost all studies of exoplanet atmospheric circulation have focussed on equinox conditions. However, as we have discussed in Sections 1-4, many polar vortices have strong seasonal dependence, existing only from autumn until spring. There is a clear need, therefore, for understanding the solstice and seasonally-varying properties of exoplanet atmospheric circulation.

Considering the vast numbers of planetary parameters that have a controlling influence on atmospheric dynamics (Kaspi & Showman, 2015; Guendelman & Kaspi, 2018; Read et al., 2018; Wang et al., 2018; Komacek & Abbot, 2019; Thomson & Vallis, 2019a), it is likely that polar vortex dynamical regimes exist that are far beyond what we have yet imagined.

## 7 Summary and Outlook

In this review, building on research from the 1800s to the present day, we have indicated how the observed genesis and structure of planetary polar vortices can be understood in terms of 1) basic planetary parameters which control the freely-evolving large-scale circulation, such as planetary rotation rate or atmospheric stratification, 2) global forcings such as solar forcing and obliquity, and 3) local forcing processes, such as the Martian latent heating from the condensation of atmospheric constituents. Within this framework, and the wider literature discussed throughout the review, we note the following key challenges for planetary polar vortex research in the future:

- To what extent do forcing asymmetries alter the structure of polar vortices? The largest unknowns come in the local forcings, and in some cases the forcings, such as the nature and organisation of convection on gas giants are not necessarily known (Dyudina et al., 2008; Thomson & McIntyre, 2016).
- What determines if a planet will have a polar vortex of Type I or II? Understanding what forcing mechanisms in a system can lead to multiple vortex configurations could in the future point to possible explanations of the vortex structures observed at Jupiter's poles, for instance. Understanding of how the various mechanisms interact with each other, perhaps as a function of planetary parameters, is a related and important step in understanding this question.

- What are the stabilising forces of the annular polar vortices for the planets that have them? Such structures are clear on Mars, and Titan, although the exact stabilising mechanisms are still unknown. The degree to which the Venusian polar vortex is annular is still debated.
- What is the role of atmospheric composition in defining vortex structure and evolution? This could be in terms of the effect of local gas enrichments on radiative forcing as in the case of Titan (Teanby et al., 2017), or condensation of major species providing a latent heat source as in the case of Mars (Toigo et al., 2017). Dynamical redistribution of trace species by the circulation means such processes may also play a role in the giant planets. It is therefore important to consider such effects in future GCMs.
- How far below the cloud top do the polar vortices extend in gas planets? This is even unknown for Saturn and Jupiter, where we have much greater coverage of their polar atmospheres. Focusing on convection processes in our comprehensive models will likely shed light in this area.
- Can exoplanet observations and modelling of polar vortices combine to help both communities? Some (highly uncertain) observation-derived estimates for zonal wind speeds on exoplanets exist, but in the coming decades these will increase in quantity and quality. Using theory and modelling to identify potential planets of interest will help inform observers as to where to look. In turn, better observations help improve our overall theories of polar vortex dynamics.
- What other types of polar vortex could exist in the exotic atmospheres outside our solar system? While there have been some studies where different planetary parameters, and scaling relationships, have been iterated to understand how features of polar vortices and jets depend on them (e.g. Brueshaber et al. (2019); Guendelman and Kaspi (2018)), there remains a wide parameter-space that exoplanets could exist in, and that could provide a deeper understanding of the atmospheric dynamics. Given the utility of regime diagrams for understanding dependence on parameters, we suggest that creation of regime diagrams for polar vortices be a priority for future research, showing how the properties of the vortex can be understood in terms of dimensional and non-dimensional planetary parameters.

Beyond this, there is now a clear need to place our understanding of polar vortices and their governing processes, developed for individual solar system planets, into a single dynamical framework along the lines of the three categories presented at the beginning of this summary. This is especially true now given the rapidly-increasing volume of exoplanetary data, that will be further enhanced by imminent new exoplanet-focused initiatives, such as the James Webb Space Telescope.

## References

Achterberg, R. K., Conrath, B. J., Gierasch, P. J., Flasar, F. M., & Nixon, C. A. (2008). Titan's middle-atmospheric temperatures and dynamics observed by the Cassini Composite Infrared Spectrometer. *Icarus*, *194*(1), 263–277.

Achterberg, R. K., Gierasch, P. J., Conrath, B. J., Flasar, F. M., & Nixon, C. A. (2011). Temporal variations of Titan's middle-atmospheric temperatures from 2004 to 2009 observed by Cassini/CIRS. *Icarus*, *211*, 686 - 698. doi: 10.1016/j.icarus.2010.08.009

Adriani, A., Mura, A., Orton, G., Hansen, C., Altieri, F., Moriconi, M., ... others (2018). Clusters of cyclones encircling Jupiter's poles. *Nature*, *555*(7695), 216.

Afanasyev, Y., & Wells, J. (2005, feb). Quasi-two-dimensional turbulence on the polar beta-plane: laboratory experiments. *Geophysical & Astrophysical Fluid Dynamics*, *99*(1), 1–17. Retrieved from `http://www.tandfonline.com/doi/abs/10.1080/03091920412331319513` doi: 10.1080/03091920412331319513

Afanasyev, Y. D. (2019, feb). Turbulence, Rossby Waves and Zonal Jets on

the Polar $\beta$-Plane: Experiments with Laboratory Altimetry. In *Zonal jets* (Vol. 2, pp. 152–166). Cambridge University Press. Retrieved from `https://www.cambridge.org/core/product/identifier/9781107358225{\%}23c8/type/book{\_}part` doi: 10.1017/9781107358225.008

Aguiar, A. C. B., Read, P. L., Wordsworth, R. D., Salter, T., & Yamazaki, Y. H. (2010). A laboratory model of Saturn's north polar hexagon. *Icarus*, *206*(2), 755–763.

Allers, K. N., Vos, J. M., Biller, B. A., & Williams, P. K. (2020). A measurement of the wind speed on a brown dwarf. *Science*, *368*(6487), 169–172.

Allison, M., Godfrey, D., & Beebe, R. (1990). A wave dynamical interpretation of Saturn's polar hexagon. *Science*, *247*(4946), 1061–1063.

Andrews, D., Holton, J. R., & Leovy, C. (1987). *Middle Atmosphere Dynamics*. San Diego, Calif.: Academic Press.

Andrews, D. G. (1987). On the interpretation of the eliassen-palm flux divergence. *Quarterly Journal of the Royal Meteorological Society*, *113*(475), 323–338.

Antuñano, A., del Río-Gaztelurrutia, T., Sánchez-Lavega, A., & Hueso, R. (2015). Dynamics of Saturn's polar regions. *Journal of Geophysical Research: Planets*, *120*(2), 155–176.

Antuñano, A., del Río-Gaztelurrutia, T., Sánchez-Lavega, A., Read, P. L., & Fletcher, L. N. (2019). Potential vorticity of Saturn's polar regions: Seasonality and instabilities. *Journal of Geophysical Research: Planets*, *124*(1), 186–201.

Antuñano, A., del Río-Gaztelurrutia, T., Sánchez-Lavega, A., & Rodríguez-Aseguinolaza, J. (2018). Cloud morphology and dynamics in Saturn's northern polar region. *Icarus*, *299*, 117–132.

Apai, D., Nardiello, D., & Bedin, L. R. (2021). Tess observations of the luhman 16 ab brown dwarf system: Rotational periods, lightcurve evolution, and zonal circulation. *The Astrophysical Journal*, *906*(1), 64.

Baines, K. H., Momary, T. W., Fletcher, L. N., Showman, A. P., Roos-Serote, M., Brown, R. H., ... Nicholson, P. D. (2009). Saturn's north polar cyclone and hexagon at depth revealed by Cassini/VIMS. *Planetary and Space Science*, *57*(14-15), 1671–1681.

Baldwin, M. P., Ayarzagüena, B., Birner, T., Butchart, N., Butler, A. H., Charlton-Perez, A. J., ... others (2020). Sudden stratospheric warmings. *Reviews of Geophysics*, e2020RG000708.

Baldwin, M. P., & Dunkerton, T. J. (2001). Stratospheric harbingers of anomalous weather regimes. *Science*, *294*(5542), 581–584.

Ball, E. R., Mitchell, D. M., Seviour, W. J., Thomson, S. I., & Vallis, G. K. (2021). The roles of latent heating and dust in the structure and variability of the northern martian polar vortex. *Planetary Science Journal*, *Accepted*. doi: 10.3847/PSJ/ac1ba2

Banfield, D., Conrath, B., Gierasch, P., John Wilson, R., & Smith, M. (2004). Travelling waves in the martian atmosphere from MGS TES nadir data. *Icarus*, *170*, 365 - 403. doi: 10.1016/j.icarus.2004.03.015

Bastin, M. E., & Read, P. L. (1998, feb). Experiments on the structure of baroclinic waves and zonal jets in an internally heated, rotating, cylinder of fluid. *Physics of Fluids*, *10*(2), 374–389. Retrieved from `http://aip.scitation.org/doi/10.1063/1.869530` doi: 10.1063/1.869530

Bolton, S. J., Adriani, A., Adumitroaie, V., Allison, M., Anderson, J., Atreya, S., ... others (2017). Jupiter's interior and deep atmosphere: The initial pole-to-pole passes with the Juno spacecraft. *Science*, *356*(6340), 821–825.

Brueshaber, S. R., Sayanagi, K. M., & Dowling, T. E. (2019). Dynamical regimes of giant planet polar vortices. *Icarus*, *323*, 46–61.

Butler, A. H., Sjoberg, J. P., Seidel, D. J., & Rosenlof, K. H. (2017). A sudden stratospheric warming compendium. *Earth System Science Data*, *9*(1).

Cantor, B. A., James, P. B., Caplinger, M., & Wolff, M. J. (2001). Martian dust storms: 1999 Mars Orbiter Camera observations. *Journal of Geophysical Research: Planets*, *106*(E10), 23653-23687. Retrieved from `https://agupubs.onlinelibrary.wiley.com/doi/abs/10.1029/2000JE001310` doi: https://doi.org/10.1029/2000JE001310

Carone, L., Keppens, R., & Decin, L. (2015). Connecting the dots–ii. phase changes in the climate dynamics of tidally locked terrestrial exoplanets. *Monthly Notices of the Royal Astronomical Society*, *453*(3), 2412–2437.

Carone, L., Keppens, R., Decin, L., & Henning, T. (2018). Stratosphere circulation on tidally locked exoearths. *Monthly Notices of the Royal Astronomical Society*, *473*(4), 4672–4685.

Charlton, A. J., & Polvani, L. M. (2007). A new look at stratospheric sudden warmings. part i: Climatology and modeling benchmarks. *Journal of Climate*, *20*(3), 449–469.

Charlton-Perez, A. J., Baldwin, M. P., Birner, T., Black, R. X., Butler, A. H., Calvo, N., ... others (2013). On the lack of stratospheric dynamical variability in low-top versions of the cmip5 models. *Journal of Geophysical Research: Atmospheres*, *118*(6), 2494–2505.

Charney, J. G., & Drazin, P. G. (1961). Propagation of planetary-scale disturbances from the lower into the upper atmosphere. *Journal of Geophysical Research*, *66*(1), 83–109.

Chemke, R., & Kaspi, Y. (2017). Dynamics of massive atmospheres. *The Astrophysical Journal*, *845*(1), 1.

Collins, M., & James, I. (1995). Regular baroclinic transient waves in a simplified global circulation model of the martian atmosphere. *Journal of Geophysical Research: Planets*, *100*(E7), 14421–14432.

Coustenis, A., Jennings, D. E., Achterberg, R. K., Lavvas, P., Bampasidis, G., Nixon, C. A., & Flasar, F. M. (2020, July). Titan's neutral atmosphere seasonal variations up to the end of the Cassini mission. *Icarus*, *344*, 113413. doi: 10.1016/j.icarus.2019.113413

de Pater, I., Fletcher, L. N., Luszcz-Cook, S., DeBoer, D., Butler, B., Hammel, H. B., ... Marcus, P. S. (2014). Neptune's global circulation deduced from multi-wavelength observations. *Icarus*, *237*, 211-238. doi: 10.1016/j.icarus.2014.02.030

Deem, G. S., & Zabusky, N. J. (1978). Vortex waves: Stationary" v states," interactions, recurrence, and breaking. *Physical Review Letters*, *40*(13), 859.

de Kok, R. J., Teanby, N. A., Maltagliati, L., Irwin, P. G., & Vinatier, S. (2014). HCN ice in Titan's high-altitude southern polar cloud. *Nature*, *514*(7520), 65.

de Pater, I., Sromovsky, L., Fry, P., Hammel, H. B., Baranec, C., & Sayanagi, K. M. (2015). Record-breaking storm activity on Uranus in 2014. *Icarus*, *252*, 121–128.

Domeisen, D. I. V., & Butler, A. H. (2020, December). Stratospheric drivers of extreme events at the Earth's surface. *Communications Earth and Environment*, *1*(1), 59. doi: 10.1038/s43247-020-00060-z

Dritschel, D. G. (1986). The nonlinear evolution of rotating configurations of uniform vorticity. *Journal of Fluid Mechanics*, *172*, 157–182.

Dritschel, D. G., & Polvani, L. M. (1992). The roll-up of vorticity strips on the surface of a sphere. *J. Fluid Mech.*, *234*, 47–69. doi: 10.1017/S0022112092000697

Dyudina, U. A., Ingersoll, A. P., Ewald, S. P., Vasavada, A. R., West, R. A., Baines, K. H., ... others (2009). Saturn's south polar vortex compared to other large vortices in the solar system. *Icarus*, *202*(1), 240–248.

Dyudina, U. A., Ingersoll, A. P., Ewald, S. P., Vasavada, A. R., West, R. A., Del Genio, A. D., ... others (2008). Dynamics of Saturn's south polar vortex. *Science*, *319*(5871), 1801–1801.

Edson, A., Lee, S., Bannon, P., Kasting, J. F., & Pollard, D. (2011). Atmospheric circulations of terrestrial planets orbiting low-mass stars. *Icarus*, *212*(1), 1–13.

Farman, J. C., Gardiner, B. G., & Shanklin, J. D. (1985). Large losses of total ozone in antarctica reveal seasonal clox/nox interaction. *Nature*, *315*(6016), 207.

Fauchez, T. J., Turbet, M., Wolf, E. T., Boutle, I., Way, M. J., Del Genio, A. D., ... others (2020). Trappist-1 habitable atmosphere intercomparison (thai). motivations and protocol version 1.0. *arXiv preprint arXiv:2002.10950*.

Fine, K., Cass, A., Flynn, W., & Driscoll, C. (1995). Relaxation of 2d turbulence to vortex crystals. *Physical review letters*, *75*(18), 3277.

Flasar, F., & Achterberg, R. (2008). The structure and dynamics of Titan's middle atmosphere. *Philosophical Transactions of the Royal Society A: Mathematical, Physical and Engineering Sciences*, *367*(1889), 649–664.

Flasar, F. M., Kunde, V. G., Abbas, M. M., Achterberg, R. K., Ade, P., Barucci, A., ... Taylor, F. W. (2004). Exploring the Saturn system in the thermal infrared: The Composite Infrared Spectrometer. *Space Science Reviews*, *115*, 169–297.

Fletcher, L., Irwin, P., Orton, G., Teanby, N., Achterberg, R., Bjoraker, G., ... others (2008). Temperature and composition of Saturn's polar hot spots and hexagon. *Science*, *319*(5859), 79–81.

Fletcher, L. N., Hesman, B., Achterberg, R., Irwin, P., Bjoraker, G., Gorius, N., ... others (2012). The origin and evolution of Saturn's 2011–2012 stratospheric vortex. *Icarus*, *221*(2), 560–586.

Fletcher, L. N., Irwin, P., Sinclair, J., Orton, G., Giles, R., Hurley, J., ... Bjoraker, G. (2015). Seasonal evolution of Saturn's polar temperatures and composition. *Icarus*, *250*, 131–153.

Fletcher, L. N., Orton, G. S., Sinclair, J. A., Guerlet, S., Read, P. L., Antuñano, A., ... Calcutt, S. B. (2018, September). A hexagon in Saturn's northern stratosphere surrounding the emerging summertime polar vortex. *Nature Communications*, *9*, 3564. doi: 10.1038/s41467-018-06017-3

Fultz, D., Long, R. R., Owens, G. V., Bohan, W., Kaylor, R., & Weil, J. (1959). Studies of thermal convection in a rotating cylinder with some implications for large-scale atmospheric motions. In *Studies of thermal convection in a rotating cylinder with some implications for large-scale atmospheric motions* (pp. 1–104). Springer.

Garate-Lopez, I., Hueso, R., Sánchez-Lavega, A., & García Muñoz, A. (2016). Potential vorticity of the south polar vortex of Venus. *Journal of Geophysical Research: Planets*, *121*(4), 574–593.

Garate-Lopez, I., Hueso, R., Sánchez-Lavega, A., Peralta, J., Piccioni, G., & Drossart, P. (2013). A chaotic long-lived vortex at the southern pole of Venus. *Nature Geoscience*, *6*(4), 254.

Garate-Lopez, I., Muñoz, A. G., Hueso, R., & Sánchez-Lavega, A. (2015). Instantaneous three-dimensional thermal structure of the south polar vortex of Venus. *Icarus*, *245*, 16–31.

Gerber, E. P., & Polvani, L. M. (2009). Stratosphere–troposphere coupling in a relatively simple agcm: The importance of stratospheric variability. *Journal of Climate*, *22*(8), 1920–1933.

Gierasch, P., Goody, R., Young, R., Crisp, D., Edwards, C., Kahn, R., ... others (1997). The general circulation of the Venus atmosphere: An assessment. *Venus II*, 459–500.

Godfrey, D. A. (1988). A hexagonal feature around Saturn's north pole. *Icarus*, *76*(2), 335–356. doi: 10.1016/0019-1035(88)90075-9

Greybush, S. J., Wilson, R. J., Hoffman, R. N., Hoffman, M. J., Miyoshi, T., Ide, K., ... Kalnay, E. (2012). Ensemble Kalman filter data assimilation of Thermal Emission Spectrometer temperature retrievals into a Mars GCM. *J. Geophys. Res. Planets*, *117*, E11008. doi: 10.1029/2012JE004097

Guendelman, I., & Kaspi, Y. (2018). An axisymmetric limit for the width of the hadley cell on planets with large obliquity and long seasonality. *Geophysical Research Letters*, *45*(24), 13–213.

Gutenberg, B. (1949). New data on the lower stratosphere. *Bulletin of the American Meteorological Society*, *30*(2), 62–64.

Guzewich, S. D., Toigo, A., & Waugh, D. (2016). The effect of dust on the martian polar vortices. *Icarus*, *278*, 100 - 118. doi: 10.1016/j.icarus.2016.06.009

Haberle, R. M., Clancy, R. T., Forget, F., Smith, M. D., & Zurek, R. W. (2017). *The atmosphere and climate of mars*. Cambridge University Press.

Haberle, R. M., Houben, H., Barnes, J. R., & Young, R. E. (1997). A simplified three-dimensional model for martian climate studies. *Journal of Geophysical Research: Planets*, *102*(E4), 9051–9067.

Hart, J. E. (1972, may). A laboratory study of baroclinic instability. *Geophysical Fluid Dynamics*, *3*(3), 181–209. Retrieved from `https://www.tandfonline.com/doi/full/10.1080/03091927208236080` doi: 10.1080/03091927208236080

Haynes, P., & McIntyre, M. (1990). On the conservation and impermeability theorems for potential vorticity. *Journal of the atmospheric sciences*, *47*(16), 2021–2031.

Held, I. M., & Hou, A. Y. (1980). Nonlinear axially symmetric circulations in a nearly inviscid atmosphere. *Journal of the Atmospheric Sciences*, *37*(3), 515–533.

Held, I. M., & Suarez, M. J. (1994). A proposal for the intercomparison of the dynamical cores of atmospheric general circulation models. *Bulletin of the American Meteorological Society*, *75*(10), 1825 - 1830. doi: 10.1175/1520-0477(1994)075⟨1825:APFTIO⟩2.0.CO;2

Hide, R. (1953). Some experiments on thermal convection in a rotating liquid. *Quarterly Journal of the Royal Meteorological Society*, *79*(339), 161–161.

Hide, R., & Mason, P. (1970, nov). Baroclinic waves in a rotating fluid subject to internal heating. *Philosophical Transactions of the Royal Society of London. Series A, Mathematical and Physical Sciences*, *268*(1186), 201–232. Retrieved from `https://royalsocietypublishing.org/doi/10.1098/rsta.1970.0073` doi: 10.1098/rsta.1970.0073

Hide, R., & Mason, P. (1975). Sloping convection in a rotating fluid. *Advances in Physics*, *24*(1), 47–100.

Holmes, J. A., Lewis, S. R., & Patel, M. R. (2020). OpenMARS: A global record of martian weather from 1999 to 2015. *Plan. and Space Sci.*, *188*, 104962. doi: 10.1016/j.pss.2020.104962

Hoskins, B. J., McIntyre, M., & Robertson, A. W. (1985). On the use and significance of isentropic potential vorticity maps. *Quarterly Journal of the Royal Meteorological Society*, *111*(470), 877–946.

Irwin, P. G. J., Fletcher, L. N., Tice, D., Owen, S. J., Orton, G. S., Teanby, N. A., & Davis, G. R. (2016). Time variability of Neptune's horizontal and vertical cloud structure revealed by VLT/SINFONI and Gemini/NIFS from 2009 to 2013. *Icarus*, *271*, 418-437. doi: 10.1016/j.icarus.2016.01.015

Ivy, D. J., Solomon, S., Calvo, N., & Thompson, D. W. (2017). Observed connections of arctic stratospheric ozone extremes to northern hemisphere surface climate. *Environmental Research Letters*, *12*(2), 024004.

Jucker, M., Fueglistaler, S., & Vallis, G. K. (2014). Stratospheric sudden warmings in an idealized gcm. *Journal of Geophysical Research: Atmospheres*, *119*(19), 11–054.

Juckes, M. (1989). A shallow water model of the winter stratosphere. *J. Atmos. Sci.*, *46*, 2934-2956. doi: 10.1175/1520-0469(1989)046⟨2934:ASWMOT⟩2.0.CO;2

Kang, W., & Tziperman, E. (2017). More frequent sudden stratospheric warming events due to enhanced mjo forcing expected in a warmer climate. *Journal of*

*Climate*, *30*(21), 8727–8743.

Karkoschka, E. (2015). Uranus' southern circulation revealed by Voyager 2: Unique characteristics. *Icarus*, *250*, 294–307.

Kaspi, Y., & Showman, A. P. (2015). Atmospheric dynamics of terrestrial exoplanets over a wide range of orbital and atmospheric parameters. *The Astrophysical Journal*, *804*(1), 60.

Kida, S. (1981). Motion of an elliptic vortex in a uniform shear flow. *Journal of the Physical Society of Japan*, *50*(10), 3517–3520.

Kidston, J., Scaife, A. A., Hardiman, S. C., Mitchell, D. M., Butchart, N., Baldwin, M. P., & Gray, L. J. (2015). Stratospheric influence on tropospheric jet streams, storm tracks and surface weather. *Nature Geoscience*, *8*(6), 433.

Kirchhoff, G. R. (1876). *Vorlesungen über mathematische physik: mechanik* (Vol. 1). Teubner.

Kolstad, E. W., Breiteig, T., & Scaife, A. A. (2010). The association between stratospheric weak polar vortex events and cold air outbreaks in the northern hemisphere. *Quarterly Journal of the Royal Meteorological Society*, *136*(649), 886–893.

Komacek, T. D., & Abbot, D. S. (2019). The atmospheric circulation and climate of terrestrial planets orbiting sun-like and m dwarf stars over a broad range of planetary parameters. *The Astrophysical Journal*, *871*(2), 245.

Krüger, K., Naujokat, B., & Labitzke, K. (2005). The unusual midwinter warming in the southern hemisphere stratosphere 2002: A comparison to northern hemisphere phenomena. *Journal of the atmospheric sciences*, *62*(3), 603–613.

Lait, L. (1994). An alternative form for potential vorticity. *J. Atmos. Sci.*, *51*, 1754–1759.

Lam, J. S.-L., & Dritschel, D. G. (2001). On the beta-drift of an initially circular vortex patch. *Journal of Fluid Mechanics*, *436*, 107–129.

Lebonnois, S., Burgalat, J., Rannou, P., & Charnay, B. (2012). Titan global climate model: a new 3-dimensional version of the IPSL Titan GCM. , *218*, 707–722.

Lee, C., Lewis, S. R., & Read, P. L. (2007). Superrotation in a Venus general circulation model. *Journal of Geophysical Research: Planets*, *112*(E4).

Lee, C., Lewis, S. R., & Read, P. L. (2010). A bulk cloud parameterization in a Venus general circulation model. *Icarus*, *206*(2), 662–668.

Li, C., Ingersoll, A. P., Klipfel, A. P., & Brettle, H. (2020). Modeling the stability of polygonal patterns of vortices at the poles of Jupiter as revealed by the Juno spacecraft. *Proceedings of the National Academy of Sciences*.

Limaye, S. S., Kossin, J. P., Rozoff, C., Piccioni, G., Titov, D. V., & Markiewicz, W. J. (2009). Vortex circulation on Venus: Dynamical similarities with terrestrial hurricanes. *Geophysical Research Letters*, *36*(4).

Limaye, S. S., & Suomi, V. E. (1981). Cloud motions on venus: Global structure and organization. *Journal of the Atmospheric Sciences*, *38*(6), 1220–1235.

Lindgren, E., Sheshadri, A., & Plumb, R. (2018). Sudden stratospheric warming formation in an idealized general circulation model using three types of tropospheric forcing. *Journal of Geophysical Research: Atmospheres*, *123*(18), 10–125.

Liu, Y., & Scott, R. (2015). The onset of the barotropic sudden warming in a global model. *Quarterly Journal of the Royal Meteorological Society*, *141*(693), 2944–2955.

Lora, J. M., Lunine, J. I., & Russell, J. L. (2015). Gcm simulations of Titan's middle and lower atmosphere and comparison to observations. *Icarus*, *250*, 516–528.

Lora, J. M., Tokano, T., d'Ollone, J. V., Lebonnois, S., & Lorenz, R. D. (2019). A model intercomparison of Titan's climate and low-latitude environment. *Icarus*, *333*, 113–126.

Love, A. (1893). On the stability of certain vortex motions. *Proceedings of the London Mathematical Society*, *1*(1), 18–43.

Luszcz-Cook, S., de Pater, I., Ádámkovics, M., & Hammel, H. (2010). Seeing double at Neptune's south pole. *Icarus*, *208*(2), 938–944.

Luz, D., Berry, D., Piccioni, G., Drossart, P., Politi, R., Wilson, C., ... Nuccilli, F. (2011). Venus's southern polar vortex reveals precessing circulation. *Science*, *332*(6029), 577–580.

Martineau, P., Chen, G., Son, S.-W., & Kim, J. (2018). Lower-stratospheric control of the frequency of sudden stratospheric warming events. *Journal of Geophysical Research: Atmospheres*, *123*(6), 3051–3070.

Matthewman, N. J., & Esler, J. (2011). Stratospheric sudden warmings as self-tuning resonances. part i: Vortex splitting events. *Journal of the atmospheric sciences*, *68*(11), 2481–2504.

Mitchell, D., & Ball, E. (2021). Polar vortex review data. doi: https://doi.org/10.5523/bris.22xc4ls5z02y426k8raaezytkp.

Mitchell, D., Scott, R., Seviour, W., Thomson, S., Waugh, D., Teanby, N. A., & Ball, E. (2021, June). *BrisClimate/polar_vortices_planetary_atmospheres: Release of code for paper resubmission.* Zenodo. Retrieved from `https://doi.org/10.5281/zenodo.5037244` doi: 10.5281/zenodo.5037244

Mitchell, D. M., Gray, L. J., Anstey, J., Baldwin, M. P., & Charlton-Perez, A. J. (2013). The influence of stratospheric vortex displacements and splits on surface climate. *Journal of Climate*, *26*(8), 2668–2682.

Mitchell, D. M., Montabone, L., Thomson, S., & Read, P. L. (2015). Polar vortices on Earth and Mars: A comparative study of the climatology and variability from reanalyses. *Q. J. Roy. Meteor. Soc.*, *141*, 550–562. doi: 10.1002/qj.2376

Montabone, L., Marsh, K., Lewis, S. R., Read, P. L., Smith, M. D., Holmes, J., ... Pamment, A. (2014). The Mars Analysis Correction Data Assimilation (MACDA) dataset v1.0. *Geosci. Data J.*, *1*, 129–139. doi: 10.1002/gdj3.13

Montabone, L., Mitchell, D. M., Thomson, S. I., Read, P. L., & McConnochie, T. H. (2014). The martian polar vortices in the 'macda' reanalysis: Climatology and variability. In *5th international workshop on mars atmosphere: Modelling and observations, oxford (uk).* doi: https://ui.adsabs.harvard.edu/abs/2014mamo.conf.1307M/abstract

Montabone, L., Wordsworth, R., Aguiar, A., Jacoby, T., Manfrin, M., Read, P. L., ... others (2010). Barotropic instability of planetary polar vortices: Civ analysis of specific multi-lobed structures. In *Hydralab iii joint transnational access user meeting* (pp. 191–194). Retrieved from `https://hydralab.eu/uploads/proceedings/CNRS-25_Montabone.pdf`

Montabone, L., Wordsworth, R., Aguiar, A., Jacoby, T., Read, P. L., McClimans, T., & Ellingsen, I. (2010). Barotropic instability of planetary polar vortices: Concept, experimental set-up and parameter space analysis. *Proc. HYDRALAB III Joint User Meeting*, *194*, 135–138. Retrieved from `https://hydralab.eu/uploads/proceedings/NTNU-16_Montabone.pdf`

Newman, C. E., Lee, C., Lian, Y., Richardson, M. I., & Toigo, A. D. (2011). Stratospheric superrotation in the TitanWRF model. *Icarus*, *213*(2), 636–654.

Nixon, C. A., Ansty, T. M., Lombardo, N. A., Bjoraker, G. L., Achterberg, R. K., Annex, A. M., ... Flasar, F. M. (2019). Cassini Composite Infrared Spectrometer (CIRS) Observations of Titan 2004–2017. *Astrophysical Journal Supplement Series*, *244*(1), 14. doi: 10.3847/1538-4365/ab3799

O'Neill, A., Oatley, C., Charlton-Perez, A. J., Mitchell, D., & Jung, T. (2017). Vortex splitting on a planetary scale in the stratosphere by cyclogenesis on a subplanetary scale in the troposphere. *Quarterly Journal of the Royal Meteorological Society*, *143*(703), 691–705.

O'Neill, M. E., Emanuel, K. A., & Flierl, G. R. (2015). Polar vortex formation in giant-planet atmospheres due to moist convection. *Nature Geoscience*, *8*(7),

523.

O'Neill, M. E., Emanuel, K. A., & Flierl, G. R. (2016). Weak jets and strong cyclones: Shallow-water modeling of giant planet polar caps. *Journal of the Atmospheric Sciences*, *73*(4), 1841–1855.

Orton, G., & Yanamandra-Fisher, P. (2005). Saturn's temperature field from high-resolution middle-infrared imaging. *Science*, *307*(5710), 696–698.

Orton, G. S., Encrenaz, T., Leyrat, C., Puetter, R., & Friedson, A. J. (2007). Evidence for methane escape and strong seasonal and dynamical perturbations of Neptune's atmospheric temperatures. *Astronomy & Astrophysics*, *473*(1), L5–L8.

Piccialli, A., Tellmann, S., Titov, D., Limaye, S., Khatuntsev, I., Pätzold, M., & Häusler, B. (2012). Dynamical properties of the Venus mesosphere from the radio-occultation experiment VeRa onboard Venus Express. *Icarus*, *217*(2), 669–681.

Piccioni, G., Drossart, P., Sanchez-Lavega, A., Hueso, R., Taylor, F., Wilson, C., ... others (2007). South-polar features on Venus similar to those near the north pole. *Nature*, *450*(7170), 637.

Polvani, L. M., & Dritschel, D. G. (1993). Wave and vortex dynamics on the surface of a sphere. *Journal of Fluid Mechanics*, *255*, 35–64.

Polvani, L. M., & Kushner, P. J. (2002). Tropospheric response to stratospheric perturbations in a relatively simple general circulation model. *Geophysical Research Letters*, *29*(7), 18–1.

Polvani, L. M., & Plumb, R. A. (1992). Rossby wave breaking, microbreaking, filamentation, and secondary vortex formation: The dynamics of a perturbed vortex. *Journal of the atmospheric sciences*, *49*(6), 462–476.

Polvani, L. M., Waugh, D., & Plumb, R. A. (1995). On the subtropical edge of the stratospheric surf zone. *Journal of the atmospheric sciences*, *52*(9), 1288–1309.

Rayleigh, J. W. S. (1880). On the stability or instability of certain fluid motions. *Proc. London Math. Soc.*, *11*, 57–72.

Read, P. (2011). Dynamics and circulation regimes of terrestrial planets. *Planetary and Space Science*, *59*(10), 900–914.

Read, P. L., & Lebonnois, S. (2018). Superrotation on Venus, on Titan, and elsewhere. *Annual Review of Earth and Planetary Sciences*, *46*, 175–202.

Read, P. L., Tabataba-Vakili, F., Wang, Y., Augier, P., Lindborg, E., Valeanu, A., & Young, R. M. (2018). Comparative terrestrial atmospheric circulation regimes in simplified global circulation models. part ii: Energy budgets and spectral transfers. *Quarterly Journal of the Royal Meteorological Society*, *144*(717), 2558–2576.

Read, P. L., Yamazaki, Y., Lewis, S., Williams, P., Miki-Yamazaki, K., Sommeria, J., ... Fincham, A. (2004). Jupiter's and Saturn's convectively driven banded jets in the laboratory. *Geophysical Research Letters*, *31*(22), L22701. Retrieved from `http://doi.wiley.com/10.1029/2004GL020106` doi: 10.1029/2004GL020106

Reinaud, J. N., & Dritschel, D. G. (2019). The stability and nonlinear evolution of quasi-geostrophic toroidal vortices. *J. Fluid Mech.*, *863*, 60–78. doi: 10.1017/jfm.2018.1013

Rong, P.-P., & Waugh, D. W. (2004). Vacillations in a shallow-water model of the stratosphere. *Journal of the Atmospheric Sciences*, *61*(10), 1174 - 1185. Retrieved from `https://journals.ametsoc.org/view/journals/atsc/61/10/1520-0469_2004_061_1174_viasmo_2.0.co_2.xml` doi: 10.1175/1520-0469(2004)061⟨1174:VIASMO⟩2.0.CO;2

Rostami, M., Zeitlin, V., & Montabone, L. (2018). On the role of spatially inhomogeneous diabatic effects upon the evolution of Mars' annular polar vortex. *Icarus*, *314*, 376–388.

Rostami, M., Zeitlin, V., & Spiga, A. (2017). On the dynamical nature of Saturn's North Polar hexagon. *Icarus*, *297*, 59–70. Retrieved from http://dx.doi.org/10.1016/j.icarus.2017.06.006 doi: 10.1016/j.icarus.2017.06.006

Sánchez-Lavega, A., Lebonnois, S., Imamura, T., Read, P., & Luz, D. (2017). The atmospheric dynamics of Venus. *Space Science Reviews*, *212*(3), 1541–1616.

Sanders, R. (2017). Keck observations reveal complex face of Uranus. *Berkeley News (Berkeley, CA) (2012)*.

Sanz-Requena, J., Pérez-Hoyos, S., Sánchez-Lavega, A., Antuñano, A., & Irwin, P. G. (2018). Haze and cloud structure of Saturn's north pole and hexagon wave from Cassini/ISS imaging. *Icarus*, *305*, 284–300.

Sayanagi, K. M., Baines, K. H., Dyudina, U., Fletcher, L. N., Sánchez-Lavega, A., & West, R. A. (2018). Saturn's polar atmosphere. *Saturn in the 21st Century*, *20*, 337.

Sayanagi, K. M., Blalock, J. J., Dyudina, U. A., Ewald, S. P., & Ingersoll, A. P. (2017). Cassini ISS observation of Saturn's north polar vortex and comparison to the south polar vortex. *Icarus*, *285*, 68–82.

Schecter, D., Dubin, D., Fine, K., & Driscoll, C. (1999). Vortex crystals from 2d euler flow: Experiment and simulation. *Physics of Fluids*, *11*(4), 905–914.

Scherhag, R. (1952). Die explosionartigen stratospharenwarmungen des spatwinters 1951-1952. *Ber. Deut. Wetterd.*, *6*, 51–63.

Schoeberl, M. R., & Hartmann, D. L. (1991). The dynamics of the stratospheric polar vortex and its relation to springtime ozone depletions. *Science*, *251*(4989), 46–52.

Scott, R. (2011). Polar accumulation of cyclonic vorticity. *Geophysical & Astrophysical Fluid Dynamics*, *105*(4-5), 409–420.

Scott, R. K., & Polvani, L. M. (2006). Internal variability of the winter stratosphere. part i: Time-independent forcing. *J. Atmos. Sci.*, *63*(11), 2758-2776. doi: 10.1175/JAS3797.1

Scott, R. K., Seviour, W. J. M., & Waugh, D. W. (2020). Forcing of the martian polar annulus by hadley cell transport and latent heating. *Q. J. R. Meteorol. Soc*, *146*, 2174–2190. doi: 10.1002/qj.3786

Seviour, W. J. M., Gray, L. J., & Mitchell, D. M. (2016). Stratospheric polar vortex splits and displacements in the high-top cmip5 climate models. *Journal of Geophysical Research: Atmospheres*, *121*(4), 1400–1413.

Seviour, W. J. M., Waugh, D. W., & Scott, R. K. (2017). The stability of Mars's annular polar vortex. *J. Atmos. Sci*, *74*(5), 1533-1547. doi: 10.1175/JAS-D-16-0293.1

Sharkey, J., Teanby, N. A., Sylvestre, M., Mitchell, D. M., Seviour, W. J., Nixon, C. A., & Irwin, P. G. (2020a). Mapping the zonal structure of Titan's northern polar vortex. *Icarus*, *337*, 113441.

Sharkey, J., Teanby, N. A., Sylvestre, M., Mitchell, D. M., Seviour, W. J., Nixon, C. A., & Irwin, P. G. (2020b). Potential vorticity structure of Titan's polar vortices from Cassini CIRS observations. *Icarus*, 114030.

Shell, K. M., & Held, I. M. (2004). Abrupt transition to strong superrotation in an axisymmetric model of the upper troposphere. *Journal of the atmospheric sciences*, *61*(23), 2928–2935.

Sheshadri, A., Plumb, R. A., & Gerber, E. P. (2015). Seasonal variability of the polar stratospheric vortex in an idealized agcm with varying tropospheric wave forcing. *Journal of the Atmospheric Sciences*, *72*(6), 2248–2266.

Showman, A. P., Cho, J. Y., & Menou, K. (2010). Atmospheric circulation of exoplanets. *Exoplanets*, *526*, 471–516.

Spence, T. W., & Fultz, D. (1977, aug). Experiments on Wave-Transition Spectra and Vacillation in an Open Rotating Cylinder. *Journal of the Atmospheric Sciences*, *34*(8), 1261–1285. Retrieved from http://journals.ametsoc.org/doi/10.1175/1520-0469(1977)034{\%}3C1261:EOWTSA{\%}3E2.0.CO;2 doi:

10.1175/1520-0469(1977)034⟨1261:EOWTSA⟩2.0.CO;2

Sromovsky, L., de Pater, I., Fry, P., Hammel, H., & Marcus, P. (2015). High s/n Keck and Gemini AO imaging of Uranus during 2012–2014: new cloud patterns, increasing activity, and improved wind measurements. *Icarus*, *258*, 192–223.

Sromovsky, L., Hammel, H., de Pater, I., Fry, P., Rages, K., Showalter, M., ... others (2012). Episodic bright and dark spots on Uranus. *Icarus*, *220*(1), 6–22.

Sugimoto, N., Kouyama, T., & Takagi, M. (2019). Impact of data assimilation on thermal tides in the case of Venus Express wind observation. *Geophysical Research Letters*, *46*(9), 4573–4580.

Suomi, V. (1974). The dynamical regime as revealed by the uv markings. In *Bulletin of the american astronomical society* (Vol. 6, p. 386).

Suomi, V. E., & Limaye, S. S. (1978). Venus: Further evidence of vortex circulation. *Science*, *201*(4360), 1009–1011.

Sylvestre, M., Teanby, N. A., Vatant d'Ollone, J., Vinatier, S., Bézard, B., Lebonnois, S., & Irwin, P. G. J. (2020). Seasonal evolution of temperatures in Titan's lower stratosphere. *Icarus*, *344*, 113188. doi: 10.1016/j.icarus.2019.02.003

Tan, X., & Showman, A. P. (2021). Atmospheric circulation of brown dwarfs and directly imaged exoplanets driven by cloud radiative feedback: global and equatorial dynamics. *Monthly Notices of the Royal Astronomical Society*.

Taylor, Diner, D., Elson, L., Hanner, M., McCleese, D., Martonchik, J., ... others (1979). Infrared remote sounding of the middle atmosphere of Venus from the Pioneer orbiter. *Science*, *203*(4382), 779–781.

Taylor, F. W. (2010). Planetary atmospheres. *Meteorological Applications*, *17*(4), 393–403.

Taylor, F. W. (2014). *The scientific exploration of venus*. Cambridge University Press.

Teanby, N., de Kok, R., Irwin, P., Osprey, S., Vinatier, S., Gierasch, P., ... others (2008). Titan's winter polar vortex structure revealed by chemical tracers. *Journal of Geophysical Research: Planets*, *113*(E12).

Teanby, N. A., Bézard, B., Vinatier, S., Sylvestre, M., Nixon, C. A., Irwin, P. G., ... Flasar, F. M. (2017). The formation and evolution of Titan's winter polar vortex. *Nature communications*, *8*(1), 1586.

Teanby, N. A., Irwin, P. G. J., de Kok, R., & Nixon, C. A. (2009). Dynamical implications of seasonal and spatial variations in Titan's stratospheric composition. *Philosophical Transactions of the Royal Society of London Series A*, *367*(1889), 697–711. doi: 10.1098/rsta.2008.0164

Teanby, N. A., Irwin, P. G. J., Nixon, C. A., de Kok, R., Vinatier, S., Coustenis, A., ... Flasar, F. M. (2012). Active upper-atmosphere chemistry and dynamics from polar circulation reversal on Titan. , *491*, 732–735. doi: 10.1038/nature11611

Teanby, N. A., Sylvestre, M., Sharkey, J., Nixon, C. A., Vinatier, S., & Irwin, P. G. J. (2019). Seasonal evolution of Titan's stratosphere during the Cassini mission. *Geophys. Res. Letters*, *46*(6), 3079–3089. doi: 10.1029/2018GL081401

Thompson, D. W., Solomon, S., Kushner, P. J., England, M. H., Grise, K. M., & Karoly, D. J. (2011). Signatures of the antarctic ozone hole in southern hemisphere surface climate change. *Nature Geoscience*, *4*(11), 741–749.

Thomson, J. J. (1883). *A treatise on the motion of vortex rings: an essay to which the adams prize was adjudged in 1882, in the university of cambridge*. Macmillan.

Thomson, S. I., & McIntyre, M. E. (2016). Jupiter's unearthly jets: A new turbulent model exhibiting statistical steadiness without large-scale dissipation. *Journal of the Atmospheric Sciences*, *73*(3), 1119–1141.

Thomson, S. I., & Vallis, G. K. (2019a, jul). The effects of gravity on the climate and circulation of a terrestrial planet. *Quarterly Journal of the Royal Meteorological Society*, *145*(723), 2627–2640. Retrieved from `https://onlinelibrary.wiley.com/doi/abs/10.1002/qj.3582` doi: 10.1002/qj.3582

Thomson, S. I., & Vallis, G. K. (2019b). Hierarchical modeling of solar system planets with isca. *Atmosphere*, *10*(12), 803.

Toigo, A. D., Waugh, D. W., & Guzewich, S. D. (2017, January). What causes Mars' annular polar vortices? , *44*(1), 71-78. doi: 10.1002/2016GL071857

Tollefson, J., de Pater, I., Marcus, P. S., Luszcz-Cook, S., Sromovsky, L. A., Fry, P. M., ... Wong, M. H. (2018). Vertical wind shear in Neptune's upper atmosphere explained with a modified thermal wind equation. *Icarus*, *311*, 317–339.

Vinatier, S., Mathé, C., Bézard, B., Vatant d'Ollone, J., Lebonnois, S., Dauphin, C., ... Jennings, D. E. (2020). Temperature and chemical species distributions in the middle atmosphere observed during Titan's late northern spring to early summer. *Astronomy and Astrophysics*, *641*, A116. doi: 10.1051/0004-6361/202038411

Vinatier, S., Schmitt, B., Bézard, B., Rannou, P., Dauphin, C., de Kok, R., ... Flasar, F. M. (2018). Study of Titan's fall southern stratospheric polar cloud composition with Cassini/CIRS: Detection of benzene ice. *Icarus*, *310*, 89–104. doi: 10.1016/j.icarus.2017.12.040

Wang, H. (2007). Dust storms originating in the northern hemisphere during the third mapping year of Mars Global Surveyor. *Icarus*, *189*(2), 325–343.

Wang, H., & Richardson, M. I. (2015, May). The origin, evolution, and trajectory of large dust storms on Mars during Mars years 24-30 (1999-2011). , *251*, 112-127. doi: 10.1016/j.icarus.2013.10.033

Wang, Y., Read, P. L., Tabataba-Vakili, F., & Young, R. M. (2018). Comparative terrestrial atmospheric circulation regimes in simplified global circulation models. part i: From cyclostrophic super-rotation to geostrophic turbulence. *Quarterly Journal of the Royal Meteorological Society*, *144*(717), 2537–2557.

Waugh, D. W., & Dritschel, D. G. (1991). The stability of filamentary vorticity in two-dimensional geophysical vortex-dynamics models. *J. Fluid Mech.*, *231*, 575-598. doi: 10.1017/S002211209100352X

Waugh, D. W., & Polvani, L. M. (2010). Stratospheric polar vortices.

Waugh, D. W., Sobel, A. H., & Polvani, L. M. (2017). What is the polar vortex and how does it influence weather? *Bulletin of the American Meteorological Society*, *98*(1), 37–44.

Waugh, D. W., Toigo, A. D., Guzewich, S. D., Greybush, S. J., Wilson, R. J., & Montabone, L. (2016). Martian polar vortices: Comparison of reanalyses. *J. Geophys. Res. Planets*, *121*. doi: 10.1002/2016JE005093

Wood, R. B., & McIntyre, M. E. (2010). A general theorem on angular-momentum changes due to potential vorticity mixing and on potential-energy changes due to buoyancy mixing. *Journal of the atmospheric sciences*, *67*(4), 1261–1274.

Wright, C., Banyard, T., Hall, R., Hindley, N., Mitchel, D., & Seviour, W. (2021). The january 2021 sudden stratosphericwarming in aeolus and mls observations. *Weather and Climate Dynamics*, *in prep*.

Yamamoto, M., & Takahashi, M. (2006). Superrotation maintained by meridional circulation and waves in a Venus-like AGCM. *Journal of the atmospheric sciences*, *63*(12), 3296–3314.

Yamamoto, M., & Takahashi, M. (2015). Dynamics of polar vortices at cloud top and base on Venus inferred from a general circulation model: case of a strong diurnal thermal tide. *Planetary and Space Science*, *113*, 109–119.

## Acknowledgments

D.M is funded under a NERC research fellowship (NE/N014057/1). N.A.T is funded by the UK Science and Technology Facilities Council and the UK Space Agency (ST/M007715/1, ST/R000980/1, ST/R001367/1). E.B is funded by a NERC GW4+ Doctoral Training Partnership studentship from the Natural Environmental Research Council (NE/S007504/1). The authors would like to thank Norihiko Sugimoto for providing the data used to create Figure 1a, Cheng Li and Alexandra Klipfel for providing the data for Figure 8, and Michael McIntyre and Mark Hammond for useful discussions. We thank Luca Montabone and the two anonymous reviewers for their insightful and thorough reviews.

## Data Availability Statement

The atmospheric model and observation data used for the original figures in the study (Figure 1, 6 and 9) are available at the University of Bristol data repository, data.bris, via https://doi.org/10.5523/bris.22xc4ls5z02y426k8raaezytkp (D. Mitchell & Ball, 2021). For all other figures the source citation or repository is given in the caption of the figure. All plotting code is available in D. Mitchell et al. (2021).

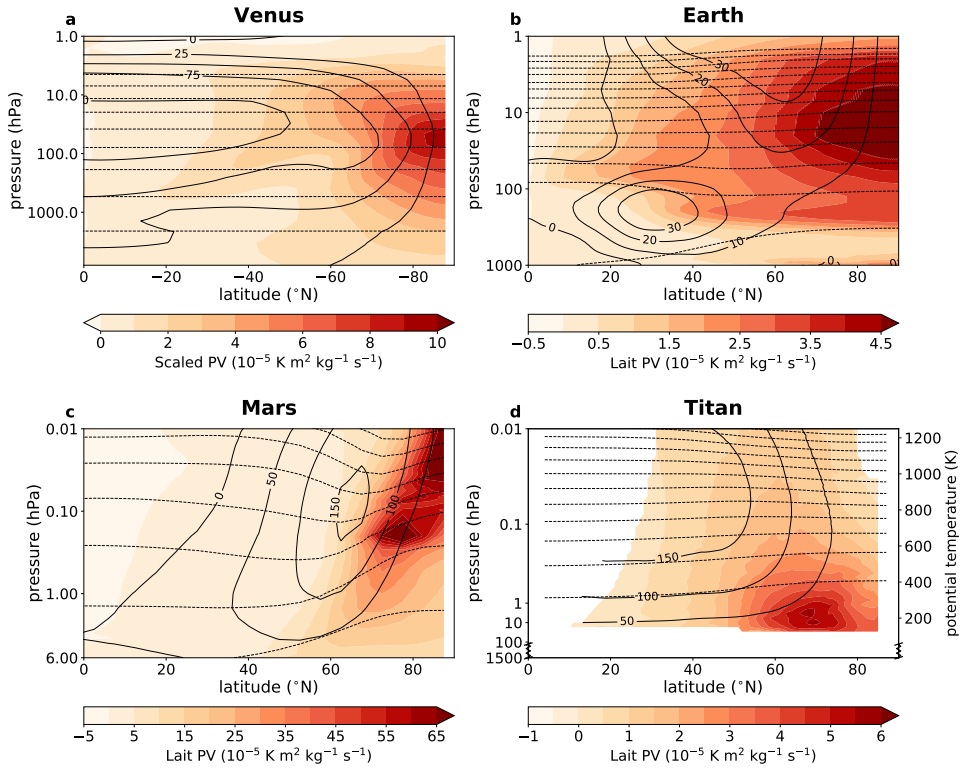


**Figure 1.** Winter zonal PV and zonal wind cross-sections as a function of altitude for Venus (a), Earth (b), Mars (c) and Titan (d). a) Southern hemisphere monthly-mean zonal-mean scaled potential vorticity (shading, scaling and PV calculations according to Piccialli et al. (2012); Garate-Lopez et al. (2016)), zonal wind (solid contours, units of ms$^{-1}$), and potential temperature (dashed contours, corresponding to 300, 400, ... K). b-d) Northern hemisphere monthly-mean zonal-mean Lait-scaled potential vorticity (shading, (Lait, 1994)), zonal wind (solid contours, units of ms$^{-1}$), and potential temperature (dashed contours, corresponding to 200, 300 ... K). Data are taken from the following sources: a) 30 Earth days (28th March - 26th April 2008) of the AFES-Venus GCM with VALEDAS data assimilation, described in Sugimoto et al. (2019); b) the ERA5 reanalysis dataset, averaged over December-January-February for 1979-2019; c) the OpenMARS reanalyis dataset, averaged over Ls 255-285° from MY 24-32; d) analysis of Cassini CIRS data from Sharkey et al. (2020b), averaged over Ls 325-345° (September 2006 - April 2008). The compressed axis represents Titan's troposphere. Note that positive winds are defined as in the direction of the rotation of the planet, which for Venus is in the opposite sense to the other planets. Figure adapted from (Waugh et al., 2016; Ball et al., 2021; Sharkey et al., 2020b; D. Mitchell & Ball, 2021)

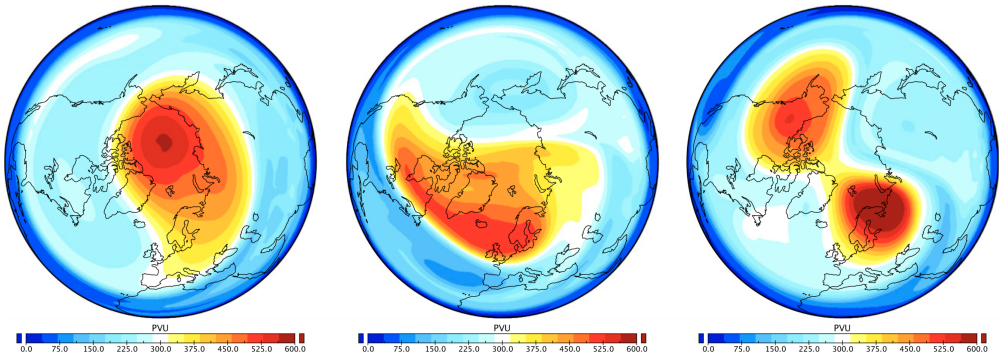


**Figure 2.** The different states of Earth's northern hemisphere stratospheric polar vortex. Northern polar stereographic plots of snapshots of Ertel (theta-normalised) potential vorticity in the mid stratosphere (10 hPa, ∼30 km) during (left) a stable period, (middle) a vortex displaced period, and (right) vortex split period. Units are Potential Vorticity Units (PVU).(Kang & Tziperman, 2017)

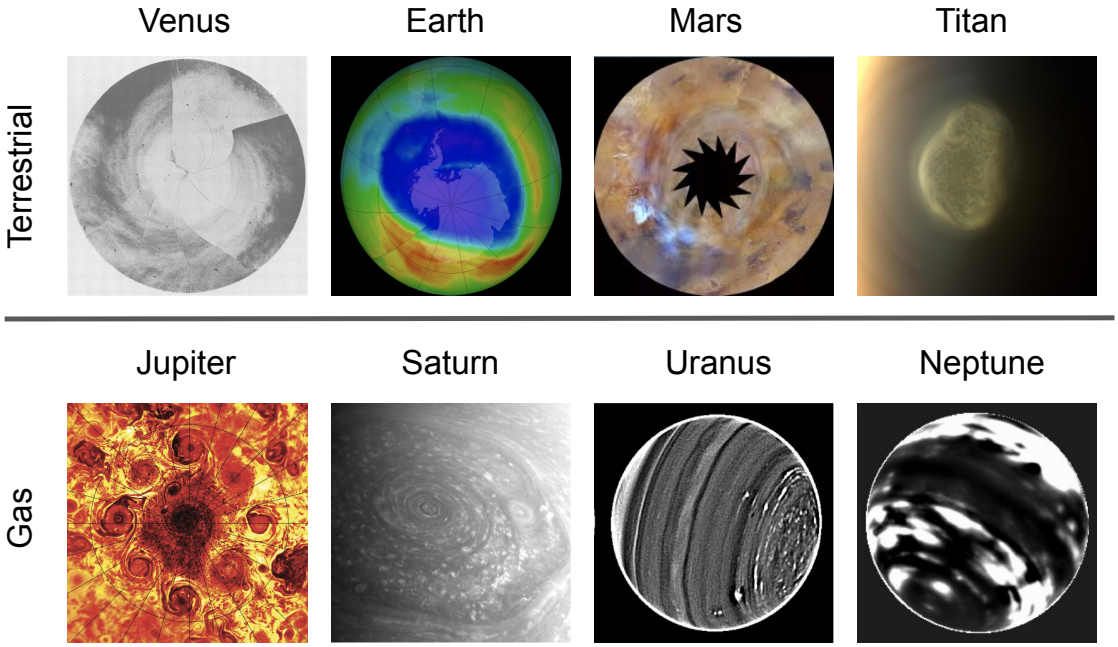


**Figure 3.** Example images which capture the varied nature of polar vortices on different planets and moons. The Venus panel shows a time-composite of images in the UV of the south polar region. The first image was taken on day 38 of 1974, and each segment of the composite shows an image taken ∼12 hours after this first (V. E. Suomi & Limaye, 1978). Earth image shows the south polar region, and is total column ozone for Sept 13, 2014 from the Ozone Monitoring Instrument (OMI) instrument on the NASA Aura satellite (*https://visibleearth.nasa.gov/images/84382/un-panel-ozone-layer-on-the-road-to-recovery/84382f*). The ozone is calculated from solar back-scatter radiation in the visible and ultraviolet. Mars image is of the northern polar region (40-90°N) taken on October the 22nd, 2012, from a MARCI/MRO colour composite, which highlights dust activity (*NASA / JPL / MSSS*). Titan image shows the south polar region, taken in false colour by ISS/Cassini (image from NASA/JPL-Caltech/Space Science Institute). Jupiter image shows the northern Type II polar vortex, taken in IR from the Juno spacecraft on the 2nd of February 2017. A latitude circle is shown at 80N (Adriani et al., 2018). The Saturn image shows the north polar region taken in the visible with ISS/Cassini (*NASA/JPL-Caltech/Space Science Institute*). Uranus image shows the north polar region (∼100° clockwise of the centre) as an enhanced adaptive optics near-IR image from the Keck II telescope, taken on 26th of July, 2012 (Sromovsky et al., 2015). Neptune image is an enhanced near-IR H-band adaptive optics image from the Keck II telescope, taken on July 3rd, 2013 (Tollefson et al., 2018).

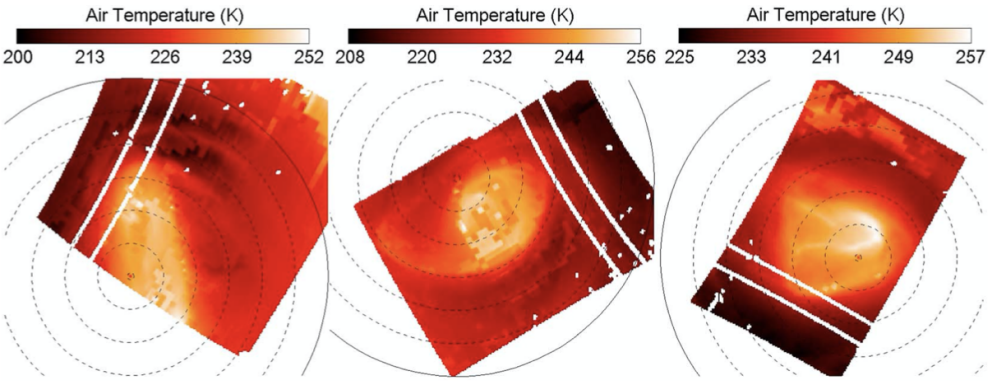


**Figure 4.** The air-temperature of the 330K isentropic surface of the southern hemisphere on Venus showing the vortex core (brighter regions) and wider vortex structure (darker regions). This is around the upper cloud level (∼58 km). The panels show data derived from three different orbits of the Venus Express, which are orbits (left) 038, (middle) 310, and (right) 475. The estimated error is about 9 K on average. Latitude circles are plotted at 5° intervals from the south pole. The white pixels and lines are due to the lack of thermal information. Figure from Garate-Lopez et al. (2016).

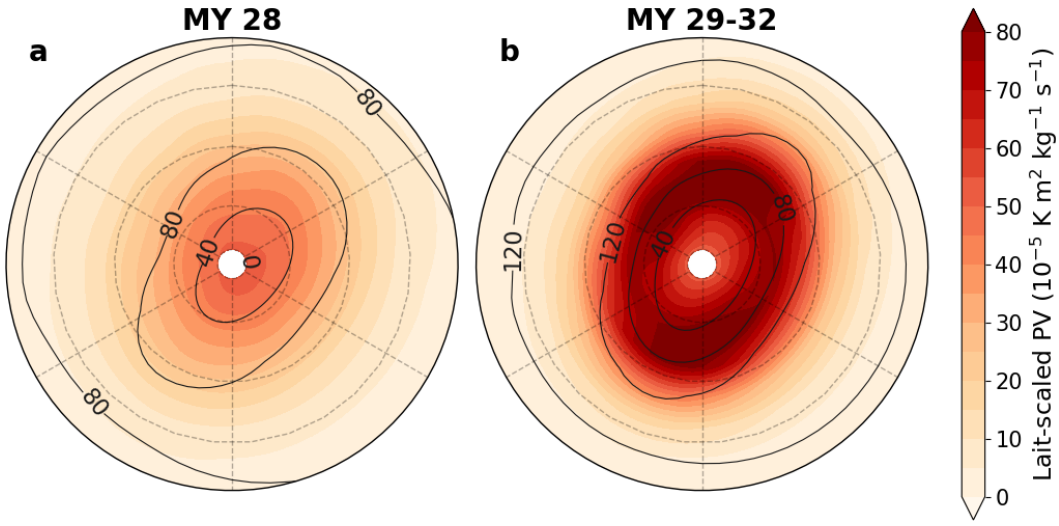


**Figure 5.** Mars' northern hemisphere polar vortex during a dust storm. Northern polar stereographic winter averages of Lait-scaled potential vorticity (shading) and zonal winds (contours) on the 350K potential temperature surface. (a) The polar vortex during the Martian Year (MY) 28 global dust storm, and (b) the polar vortex averaged over MY 29-32, during which time there were no global dust storms. Data are extracted from the OpenMARS reanalysis dataset and averaged over $L_s$ = 255 - 285°. Panels are bounded at 50°N and dashed lines of latitude are at intervals of 10°N. Figure adapted from (Ball et al., 2021).

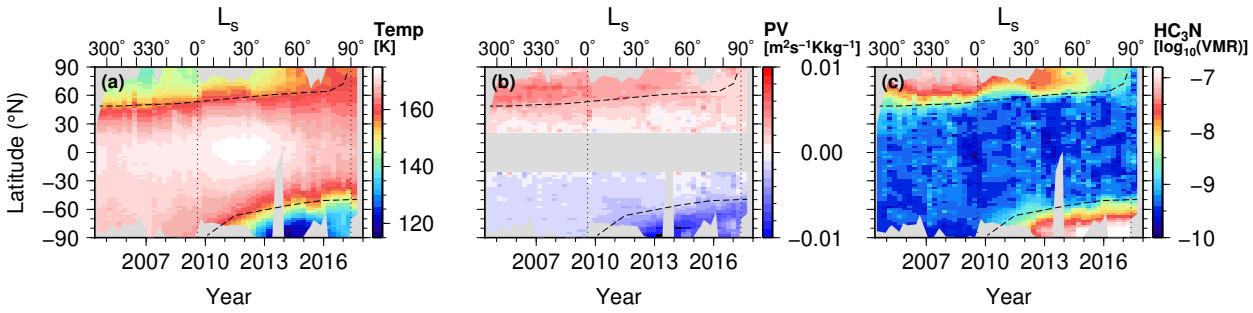


**Figure 6.** Titan's polar vortex structure and evolution observed by Cassini CIRS. (a) Temperature at 1 hPa (Sharkey et al., 2020b) showing cold mid-stratosphere temperatures within the polar vortices. (b) PV at 0.1 hPa (Sharkey et al., 2020b) showing strong PV gradients near the vortex edge and an annular PV structure, with peak PV at ∼65°. (c) $HC_3N$ volume mixing ratio (VMR) (Teanby et al., 2019) showing confinement of a short lifetime ($\ll$ a Titan year) gas withing the polar vortex. Dotted vertical lines are the 2009 northern spring equinox and 2017 northern summer solstice. Dashed regions indicate approximate edge of northern and southern vortices.

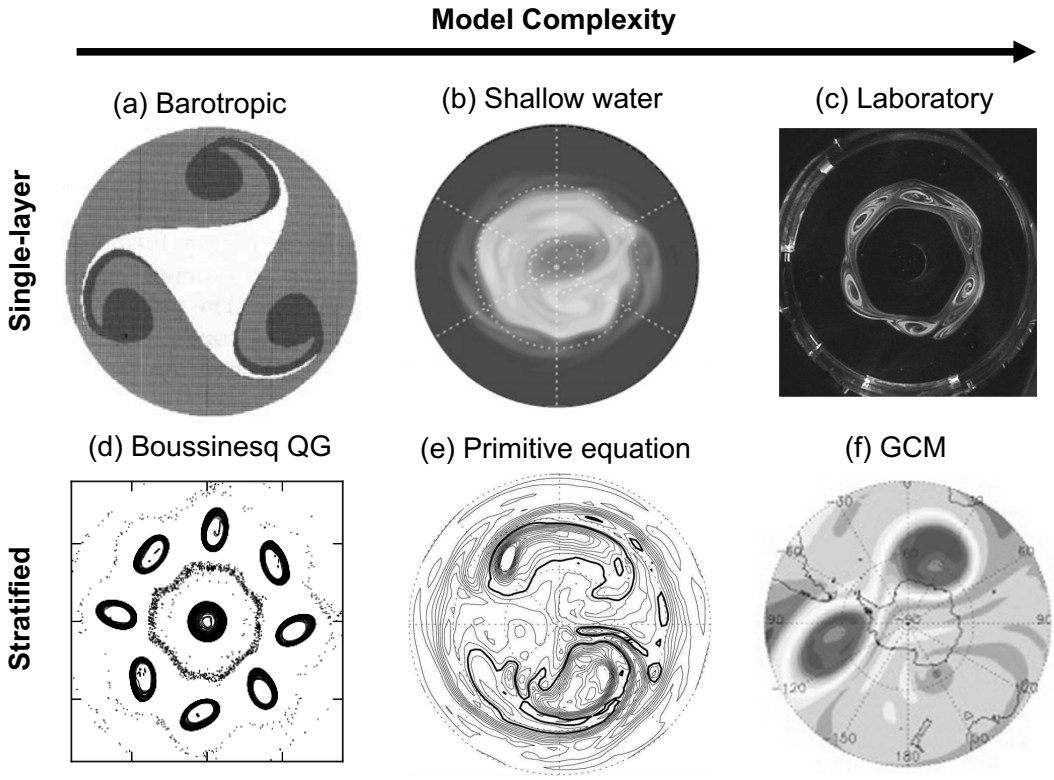


**Figure 7.** Major features of planetary polar vortices as simulated in a hierarchy of single-layer and stratified models of varying complexity. a) Instability of a Mars- or Titan-like annular vortex in a nondivergent barotropic model (Dritschel & Polvani, 1992). b) Mars-like annular polar vortex simulated in a divergent barotropic (shallow water) model with thermal relaxation (Seviour et al., 2017). c) Saturn-like hexagonal jet in a rotating tank laboratory experiment (Aguiar et al., 2010). d) Jupiter-like multiple-vortex equilibrium in a quasi-geostrophic Boussinesq simulation (Reinaud & Dritschel, 2019). e) Earth-like stratospheric polar vortex splitting event simulated in a dry primitive equation model with Newtonian relaxation of temperature (Scott & Polvani, 2006). f) Forecast of the 2002 Antarctic sudden stratospheric warming in a comprehensive GCM (A. O'Neill et al., 2017).

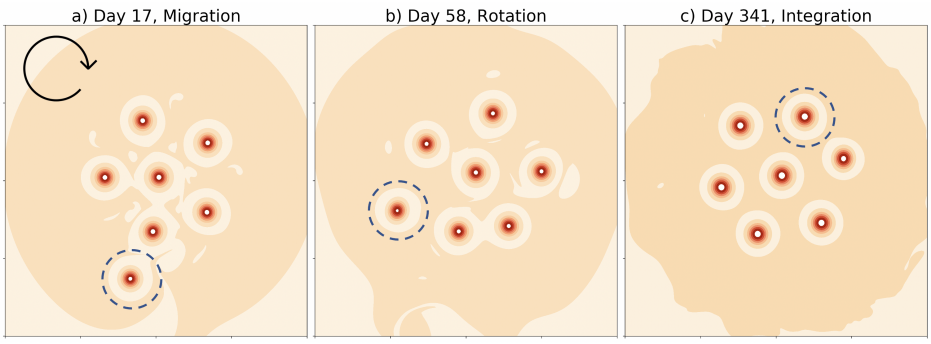


**Figure 8.** A simulation of Jupiter's vortex clusters, showing a) an intruder migrating in, b) rotation of that intruder around the main cluster, and c) integration of the intruder into the main cluster. The vortex of interest has a dashed circle around it. The direction of rotation of the configuration is given in the left panel. Figure adapted from Li et al. (2020).

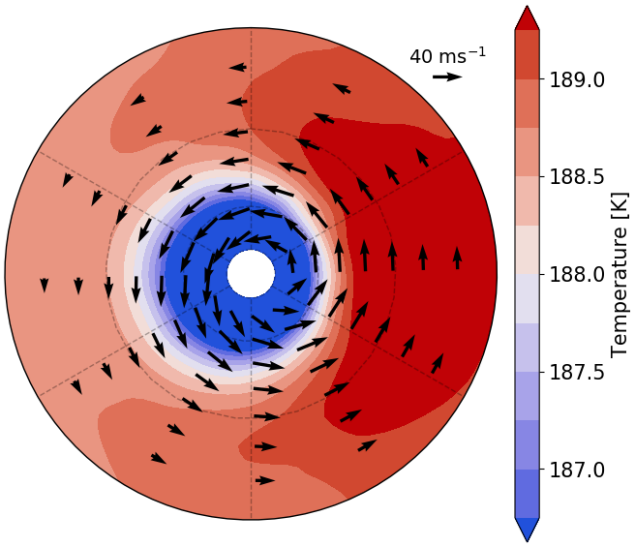


**Figure 9.** Northern polar stereographic plot of temperature (shading) and zonal wind (vectors) on the 5 hPa level from model simulations of TRAPPIST-1e. Dashed lines correspond to 30,60°N and the figure is bounded at the equator. Data is taken from the HAB1 Unified Model experiment from Fauchez et al. (2020).